Resonant Nanophotonics Educational Workshop 2024

Clover

Book of abstracts

Skoltech ITMO MIPT ACTIVE PHOTONICS

Skolkovo Institute of Science and Technology

RESONANT NANOPHOTONICS 2024
EDUCATIONAL WORKSHOP

July 8–12, 2024, Moscow

Book of abstracts

Moscow University Press, 2024

UDC 535+620.3(082)
LBC 22.343+30.3я431
R 45

Organizer

Skolkovo Institute of Science and Technology, Bolshoi boulevard 30, str. 1, Moscow, Russia

R 45 Resonant Nanophotonics Educational Workshop 2024, July 8–12, 2024, Moscow : Book of abstracts. — Moscow : Moscow University Press, 2024. — 56, [1] p. : il. (tabl.). — Electronic edition of network distribution.

ISBN 978-5-19-012128-5 (e-book)

The edition abstracts of oral and poster presentations of participants of the Resonance Nanophotonics Educational Workshop (ReNEW) conference, which was held from July 8 to 12, 2024, at the Skolkovo Institute of Science and Technology.

UDC 535+620.3(082)
LBC 22.343+30.3я431

ISBN 978-5-19-012128-5
(e-book)

Сколтех (Сколковский Институт науки и технологий)

РЕЗОНАНСНАЯ НАНОФОТОНИКА — 2024
ОБРАЗОВАТЕЛЬНЫЙ СЕМИНАР

8–12 июля 2024 года, Москва

Тезисы докладов

Издательство Московского университета
2024

УДК 535+620.3(082)
ББК 22.343+30.3я431
Р 34

Р 34 **Резонансная нанофотоника — 2024** : образовательный семинар, 8–12 июля 2024 года, Москва : Тезисы докладов. — Москва : Издательство Московского университета, 2024. — 56, [1] с. : ил. (табл.). — Электронное издание сетевого распространения.

ISBN 978-5-19-012128-5 (e-book)

Издание содержит тезисы устных и стендовых докладов участников конференции Образовательный семинар по резонансной нанофотонике (Re-NEW), которая проходила с 8 по 12 июля 2024 года в Сколковском институте науки и технологий.

УДК 535+620.3(082)
ББК 22.343+30.3я431

ISBN 978-5-19-012128-5 (e-book)

Investigation of the two-dimentional heterobilayer WS_2/WSe_2 semiconducting moiré superlattice

E. Barulina[1], E. Chiglintsev[1,2], A. Chernov[1,2]

[1]Quantum Spintronics and low-dimentional materials, Russian Quantum Center, Moscow, Russian Federation
[2]Physics of Magnetic Heterostructures and Spintronics for Energy-Efficient Technologies, Moscow Institute of Physics and Technology, Dolgoprudny, Russian Federation
e.barulina@rqc.ru

The moiré heterostructures of van der Waals materials are a promising platform for creating and investigating of new correlated states of bosons and fermions and an alternative method to achieve a wide range of highly controllable quantum Hamiltonians. The physical mechanism of a quantum interference of moiré heterostructures can be described as an analogy of classical moiré interference patterns based on formation of the combined periodic motif at longer wavelength for twisted at small angle bilayer compared to a pristine monolayer. In particular, triangular lattice twisted bilayer of WSe_2 and WS_2 describe Hubbard model demonstrated strong electron correlation due to the strong Coulomb interaction and the formation of a flat moiré miniband. During this work, the twisted WS_2/WSe_2 devices based on the Graphene/hBN/WS_2/WSe_2/hBN/Graphene structures were constructed by dry pick-up method enable interlayer excitons formation, with holes and electrons residing in the WSe_2 and WS_2, correspondingly. The effect of the rotation angle in the R (60° twisted)- and H (0° twisted)- stacked WS_2/WSe_2 moiré superlattice device's configuration were investigated. The extended natures of the interlayer excitons in the H-stacked compared to the R-stacked moiré superlattice devices were demonstrated. Future research on valley physics in strongly correlated bosonic systems is encouraged by the valley-polarized excitons, which open up new avenues for the study of correlated excitons.

Symmetry switchable quasi-BIC in dielectric cuboid

M. Bochkarev[1*], N. Solodovchenko[1], K. Samusev[1,2], M. Limonov[1,2]

[1]ITMO University, Saint-Petersburg, 197101, Russian Federation, Saint-Petersburg, Russia

[2]Ioffe Institute, Saint-Petersburg, 194021, Russian Federation, Saint-Petersburg, Russia

**e-mail address: mikhail.bochkarev@metalab.ifmo.ru*

Quasi bound states in the continuum (q-BIC) are of great interest in modern photonics, due to its potential role of a new basis for high-sensitivity sensors [1]. Such unique states occur under strong coupling regime between at least of two modes with the same symmetry group. In this case destructive interference produce a far-field radiation suppression, at the same time a strong field localized inside resonator. Recently, q-BIC was observed in finite 3D dielectric cylinders [2] and rings [3], this work expand these studies to cuboid resonator.

We considered 3D dielectric cuboid resonator, which supports different types of Fabry-Perot-like modes, each of which can be characterized by three indexes (W, H, L). Index W depicts how many half wavelengths fit in the optical width of the resonator, and the same for height (H) and length (L). We found that under certain aspect ratios between dimensions of the resonator, spectral positions of modes with indexes (1, 1, L) and (1, 3, L) can overlap and produce characteristic anti-crossing in parametric space, which is fingerprint of a q-BIC state, with increasing of Q factor for one of photonic modes. At the same time, modes with even L indices have anti-symmetric magnetic field distribution. Such peculiarity provides opportunity to forbit the excitation of both interacting modes by symmetry reasons under certain illumination conditions. Due to this, q-BIC state can be switched on or off in scattering spectra, depending on relative orientation of the resonator and incident plane wave.

For experimental verification of this effect, we use high-permittivity low-loss ceramic cuboid resonator with ε = 44.5+0.004i, length 109 mm, width 4 mm, and height 11 mm in microwave frequency range. Measurements of extinction cross section was provided with a 0.05 mm step on the height of the resonator to obtain a scattering maps for two excitation setups, depicted in Fig. 1 (a) and (b).

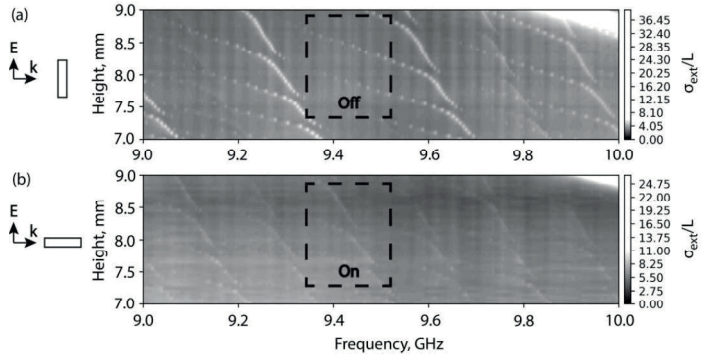

Fig. 1 Scattering maps for dielectric cuboid. (a) Wave vector of the incident wave is perpendicular to the resonator, (b) wave vector is parallel to the resonator length.

Indeed, the symmetry forbidden q-BIC are not observed for a setup in Fig. 1 (a), but such states can be «switched on» by rotation of the resonator by 90 degrees (Fig. 1 (b)). At the same time, we observe neighbor q-BIC states, which occur between symmetric modes with indexes (1, 1, L) and (1, 3, L), where L is odd number. These states cannot be forbitten by symmetry and excited in both considered excitation setups.

Notable, that one can observe a lot of q-BIC states equidistantly placed in parametric space for such structure. At least two neighbor q-BIC states can be observed for resonator with fixed parameters. Together with a such shape as a cuboid, which is easy to manufacture even in nano-meter scale, such resonators may be used for sensing and light control applications.

This work was performed with financial support of the Russian Science Foundation № 23-12-00114.

References

[1] C. W. Hsu, B. Zhen, A. D. Stone, J. D. Joannopoulos, M. Solja˘ci´c, "Bound states in the continuum". Nature Reviews Materials, **1,** 9 (2016).

[2] A. Bogdanov, K. Koshelev, P. Kapitanova, M. Rybin, S. Gladyshev, Z. Sadrieva, K. Samusev, Y. Kivshar, M. Limonov, "Bound states in the continuum and fano resonances in the strong mode coupling regime", Advanced Photonics **1**, 01 (2019).

[3] N. Solodovchenko, K. Samusev, D. Bochek, M. Limonov, "Bound states in the continuum in strong-coupling and weak-coupling regimes under the cylinder – ring transition", Nanophotonics 10 **17**, 4347–4355 (2021).

Optical study of Er^{3+} and Nd^{3+}/Yb^{3+}-doped CeO_2 and CeO_2 / CeF_3 nanoparticles.

A. Dokudovskaya[1], R. Rakhmatullin[1], O. Morozov[1,2], S. Korableva[1], V. Semashko[1,2], and M. Pudovkin[1]*

[1]*Kazan Federal University, Institute of physics, Kazan, Russian Federation*

[2] *Zavoisky Physical-Technical Institute, FRC Kazan Scientific Center of RAS, Kazan, , Russian Federation*

**e-mail address: fyz0561999@gmail.com*

Abstract— here, the facile dry synthesis of double-phase CeO_2/ CeF^3 nanoparticles doped with Er^{3+} or Nd^{3+}/Yb^{3+} ions using ammonium bifluoride (NH_4HF_2) is reported. This method allows synthesizing double-phase nanoparticles with different ratio of CeO_2 (Ce^{4+}) and CeF_3 (Ce^{3+}). The luminescence spectra show that the intensity of Ce^{3+} peak increases after fluorination revealing the fact, that the amount of CeF_3 phase is increased. In its turn, the intensity of Er^{3+} increases by 3.5 times after fluorination under Ce^{3+} excitation, confirming the above-mentioned hypothesis. In the Nd^{3+}, Yb^{3+}:CeF_3 nanoparticles, under Nd^{3+} excitation Yb^{3+} emission is not observed. However, after formation of double-phase Nd^{3+}/Yb^{3+}:CeO_2/ CeF_3 samples, both Nd^{3+} and Yb^{3+} emissions are observed.

Rare earth-based nanoparticles (NPs) are promising materials for such applications as catalysis, optoelectronics, bio-imaging [1], and temperature sensing [2]. There are numerous publications about application of both types of cerium NPs for catalysis and medical purposes. Cerium dioxide NPs (or ceria - CeO_2) has been extensively studied due to its great properties such as the oxygen storage capacity and the ability to keep its fluorite-type phase at high concentration of oxygen vacancies. These properties are due to the easy transition between Ce^{4+} and Ce^{3+} states in ceria. The presence of Ce^{4+} and Ce^{3+} ions provides redox activity of the samples. Thus, the CeO2 NPs act as anti-inflammatory agents. Prominent properties of CeO_2 and CeF_3 NPs can be combined by synthesizing double-phase CeO_2/CeF_3 NPs. In its turn, the doping procedure can increase the number of applications. For example, it could be used for temperature sensing, X-ray induced photodynamic therapy, catalysis, up and down conversion and other fields.

The purpose of my work was to study the influence of double-phase CeO2/CeF3 on the luminescent properties of Er^{3+} and Nd^{3+}, Yb^{3+}.

A. CeO_2/CeF_3: Er^{3+}

Double-phase CeO_2/CeF_3: Er^{3+} NPs were obtained by fluorination of Er^{3+}:CeO_2 NPs. As it was mentioned above, cerium has two oxidation states, 3+ and 4+, and the relative concentration of Ce^{3+} and Ce4+ depends on the redox conditions of the sample preparation process. Under Ce^{3+} excitation at 266 nm, the broad Ce^{3+} emission peak centered at ~ 440 nm is clearly seen. There is also energy transfer from Ce^{3+} to Er^{3+} via $^4F_{5/2}$ excited sate of Er^{3+}. In addition, there are non-radiative transitions from excited $^4F_{5/2}$ state to lower $^2H_{11/2}$ and 4F9/2 ones. In particular, the total intensity of 4f-4f luminescence of CeO_2/CeF_3: Er^{3+} (0.1 at.%) NPs is 3.5 time higher compared to CeO_2: Er^{3+} (0.1 at.%) one under both UV or resonant excitations. Probably it can be associated with the increased concentration of trivalent rare-

earth ions in a cubic-distorted environment and the observed phenomena require further studies. The shape of the Er^{3+} spectra is not significantly affected by the formation of double-phase sample. It can be explained by the shielded nature of the 4f shell of Er^{3+}.

B. CeF_3/CeO_2: Nd^{3+}, Yb^{3+}

In the case CeF_3/CeO_2: Nd^{3+}, Yb^{3+} NPs, there was an opposite synthesis procedure. Firstly, the single-phase CeF3: Nd^{3+}, Yb^{3+} NPs were synthesized. Here, under Nd^{3+} excitation Yb^{3+} emission is not observed. However, after annealing in air and formation of double-phase c samples, both Nd^{3+} and Yb^{3+} emissions are observed (Fig.1). In the single-phase CeO_2: Nd^{3+}, Yb^{3+} nanoparticles the Yb^{3+} emission only is observed under the same excitation conditions. This phenomenon can be related to the several factors including transformation of phonon spectrum. Temperature-dependent spectral characterization of CeF_3/CeO_2: Nd^{3+}, Yb^{3+} shoved, that they can be used in the remote luminescence temperature sensing.

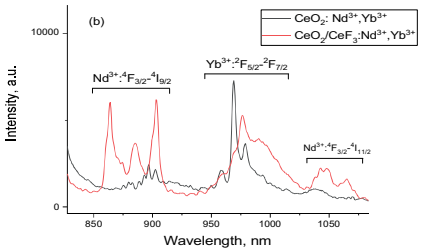

Fig. 1 Room-temperature luminescence spectra of CeF_3: Nd^{3+}, Yb^{3+}, CeF_3 /CeO_2: Nd^{3+}, Yb^{3+} and CeO_2: Nd^{3+}, Yb^{3+} NPs under excitation at λ_{ex}=790 nm.

References

[1] Chen C., Li C., Shi Z. Current advances in lanthanide-doped upconversion nanostructures for detection and bioapplication //Advanced Science. – 2016. – Т. 3. – №. 10. – С. 1600029.

[2] Ginkel A. Pudovkin, M., Oleynikova, E., Korableva, S., & Morozov, O. Optical Temperature Sensors Based on Down-Conversion Nd^{3+}, Yb^{3+}: $LiYF_4$ Microparticles //Photonics. – MDPI, 2023. – Т. 10. – №. 4. – С. 375.

Exceptional Points in Waveguides with Chiral Media

Jim A. Enriquez[1*], Pedro Torres[2]

[1] School of Physics and Engineering, ITMO University, Saint-Petersburg 197101, Russia

[2] Universidad Nacional de Colombia, Department de Física, Medellín, Colombia

**e-mail address: jim.enriquez@metalab.ifmo.ru*

We identify a simple and novel approach to implement exceptional points (EPs) in non-Hermitian systems, which offers a more versatile configuration beyond a spatially arranged optical potential. The introduction of chiral layers, consisting on a purely imaginary chirality parameter into Hamiltonians corresponding to dielectric achiral waveguides give rise to anti-PT symmetric Hamiltonians. Such non-Hermitian Hamiltonians may exhibit EPs where two eigenvalues and eigenvectors of the system coalesce simultaneously and do not require tailored platforms with controlled optical gain and loss. Importantly, our waveguide platform is a theoretical proposal, validated through numerical simulations, that can be exploited for basic research and a broad range of applications.

Non-Hermitian systems as theoretical models of open or dissipative systems exhibit rich novel physical properties and fundamental issues. Non-Hermitian photonic systems supporting anti-PT-symmetric EPs have been demonstrated, among others, using optical waveguides with imaginary couplings and off-the-shelf-component based standard telecommunication single-mode fibre [1]. The configurations mentioned above may have intrinsic difficulties in the experimental stage, especially the most common ones that require complex arrangements with controlled gain-loss interplay. This work introduces a new and simple design concept to obtain anti-PT symmetry and EPs based on the inclusion of chiral layers with a purely imaginary chirality parameter forming waveguides.

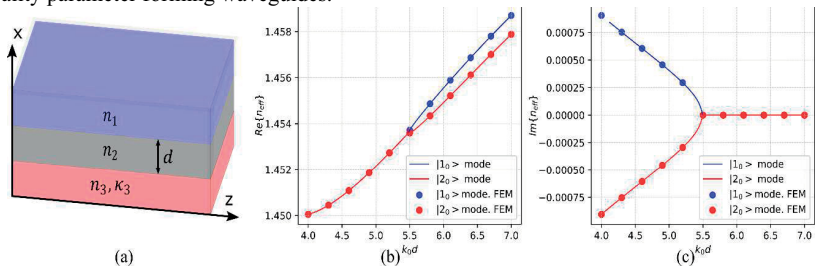

Fig. 1 Anti-PT-symmetry breaking and exceptional points in the asymmetric three-layer waveguide with isotropic chiral media. (a) Schematic of the structure. Computational and theoretical results of (b) real part of n_{eff}, and (c) imaginary part of n_{eff}.

The schematic of the asymmetric slab waveguide with a chiral medium is illustrated in Fig. 1a. We describe the hybrid modes of the waveguide as a linear combination of basis vectors represented by right- and left-circularly polarized modes, in which even asymmetries introduced by the chirality parameter in the fields can be reproduced:

$$\mathbf{\Psi} = (A_{+}\mathbf{\Psi}_{+}(x) + A_{-}\mathbf{\Psi}_{-}(x))e^{-i\beta z},$$

where β is the propagation constant of the hybrid modes, and the subscripts + and - hold for right and left circularly polarized light, respectively. This approach allows for the exact

derivation of the structure's dispersion curves [2], ultimately demonstrating the existence of EPs. As an example, the dispersion curves for the propagation modes supported by the three-layer asymmetric waveguide (see Fig. 1a) are illustrated in Figs. 1b and 1c. The following parameters were used to simulate the asymmetric structure: $n_1 = 1.33$, $n_2 = 1.48$, $n_3 = 1.45$, $\kappa_3 = 0.001i$. Our theoretical predictions and numerical simulations are in excellent agreement, both indicating the presence of exceptional points within the investigated structure. It is evident that for larger values of the normalized frequency $k_0 d > (k_0 d)_{EP}$ the eigenvalues corresponding to the eigenmodes |1> and |2> have the same imaginary part equal to zero, whereas their real parts differ. As the normalized frequency is reduced, they coalesce at an EP singularity. Below the EP, the two eigenvalues acquire different imaginary parts, manifesting a phase transition and broken symmetry.

In conclusion, this work theoretically and computationally reveals that anti-PT symmetry and its transition to a broken phase can be performed with a single three-layer waveguide containing chiral media with a purely imaginary chirality parameter and mitigated extinction coefficient.

References

[1] Bergman, A., Duggan, R., Sharma, K., Tur, M., Zadok, A., & Alù, A. (2021). Observation of anti-parity-time-symmetry, phase transitions and exceptional points in an optical fibre. *Nature communications*, *12*(1), 486.

[2] Enriquez, J. A., & Torres, P. (2023). Theoretical and computational study of the effects of the complex chirality parameter in chiral-coated planar waveguides. *JOSA B*, *40*(4), C86-C95.

Numerical Study of Second Harmonic Generation in GaP Nanowires

A. Funtikova[1*], A. Mozharov[2], I. Mukhin[1,2], V. Fedorov[1]

[1]Peter the Great St. Petersburg Polytechnic University, Saint-Petersburg 195251, Russia

[2]Alferov University, Saint-Petersburg 194021, Russia

**e-mail address: n.fn@mail.ru*

As electronic integrated circuits continue to evolve, their designers constantly seek to push these technologies to their physical limits due to the growing demands for storage capacity and faster data transmission rates. One compelling frontier in this domain is the development of optical integrated circuits, which by nature, could potentially bypass some of the inherent limitations seen in their electronic counterparts. Consequently, the advancement of integrated optical systems has moved beyond their conventional use in communication systems to the establishment of distinct areas focusing on signal multiplexing, signal filtering, applications in the development of various sensing components that leverage the nonlinear properties of the materials employed [1]. Presently, a significant trend in this domain involves the design of optical systems that facilitate frequency summing and doubling, where nonlinear crystals play a crucial role in the active part of these systems.

To achieve the necessary miniaturization required for high-density integration, nanostructures such as nanowires, quantum wires, and quantum dots are essential. Although these can be manufactured using well-established silicon technologies, the use of silicon for photonic devices comes with notable drawbacks. But the symmetric properties of the silicon lead to the zero second-order nonlinearity, which defines the opportunity of second harmonic generation (SHG) in crystals.

An alternative that offers considerable advantages is the use of III-V semiconductor materials, particularly GaP nanowires. These nanowires not only exhibit excellent crystallinity but can also be seamlessly integrated onto silicon substrates, ensuring compatibility with existing silicon technologies [2]. In the context of observing second harmonic generation, GaP nanowires emerge as a particularly advantageous material. Structural properties of GaP crystals make them an appealing choice for these applications. Their elongated, highly anisotropic shape and high value of second-order nonlinearity can enhance the efficiency of second harmonic generation due to improved alignment of crystalline structures and optimized interaction volumes for photon interaction. Also such shape can be efficiently integrated of nanowires onto silicon substrates. So, it is important to take structures' shape and orientation of the radiation source into account while modeling future possible usages.

In this work numerical study of the SHG in GaP nanowires of different diameters and different radiation source configurations was held to achieve optimal SHG direction (we define optimal SHG directions when it generates along the nanowire's length). In our research, we utilized COMSOL Multiphysics for simulating the required phenomena. The model included a mesh size of 35 nm across all geometries and configurations to minimize computational inaccuracies. To solve the system, the MUMPS (Multifrontal Massively Parallel Sparse Direct Solver) was employed. We conducted parametric sweeps, varying the

diameter of the structure and the radiation source angle, to examine all relevant configurations thoroughly. To eliminate any potential interference effects, we implemented a perfect matched layer (PML) along the external boundaries. The refractive and extinction indexes for GaP, which were essential for our calculations, were sourced from [3]. Outer shell of the model was defined as PDMS matrix with optical properties that were taken from [4].

We have demonstrated the influence of the radiation source disposition and structures' diameter on the second harmonic generation. Obtained form of the second-order nonlinear susceptibility tensor can predict radiation source angle that provides desired optimal SHG directions and it matches with <111> direction, where crystal growth direction matches with <001> direction. It was found out that it is also important to take into account not only the material's refractive index but also the refractive index of directly the structure itself. In turn, it depends on the diameter of the nanowire. It was demonstrated that the difference between real radiation source angle that provides optimal SHG direction and predicted slowly decreases with the grow in diameters. It can be explained by the approach with increasing diameters to the case of a bulk crystal.

Results of this work can be used in creation of the components with nonlinear active elements such as lasers, coherent radiation sources, frequency converters and optical amplifiers with known properties for future successful integration in circuits.

The work was supported by the Ministry of Science and Higher Education (state assignment grant FSEG-2024-0017).

References

[1] Cedric, V., Yves, C., Andre, P., "Sum Frequency Generation Spectroscopy in Biosensors Technology", Biosensors - Emerging Materials and Applications, **1**, 59 (2011).

[2] Zhang, G., Tateno, K., Sogawa, T., Nakano, H., "Growth and characterization of GaP nanowires on Si substrate", Journal of Applied Physics, **103** (1), 014301 (2008).

[3] Adachi, S., "Optical dispersion relations for GaP, GaAs, GaSb, InP, InAs, InSb, $Al_xGa_{1-x}As$, and $In_{1-x}Ga_xAs_yP_{1-y}$", Journal of Applied Physics, **66** (12), 6030–6040 (1989).

[4] X. Zhang, J. Qiu, X. Li, J. Zhao, L. Liu., "Complex refractive indices measurements of polymers in visible and near-infrared bands", Appl. Opt., **59**, 2337-2344 (2020).

FDTD-simulation of Raman scattering in a layered thin-film system with spatial dispersion

***A. R. Gazizov*[1*]**

[1]*Kazan Federal University, Institute of Physics, 420008, Russian Federation, Kazan*

**e-mail address: equus.meteores@gmail.com*

Currently, one of the problems of nanophotonics is the control of the interaction of light with individual nanoobjects and its various excitation modes. In particular, light can be used not only as a means for transmitting information in sub-wavelength structures or as a spectroscopic probe of nano-sized objects, but also to maintain a certain local temperature, for example, using the phenomena of photo-induced heating and laser cooling of a solid [1]. Controlling local temperature is especially important for selective control over the quantum state of an object. Using the optomechanical interaction of the field with the object, optical cooling can be achieved, the magnitude of which depends on the coupling parameter [2, 3].

The resulting optical forces lead to a coherent transfer of energy from mechanical vibrations into the optical field (stimulated anti-Stokes Raman scattering, SARS). On the other hand, the processes of light absorption and spontaneous Stokes scattering contribute to the transfer of energy from the optical field to vibration, which negatively affects the cooling efficiency. The problem of optomechanical interaction of light with propagating solid-state phonons is also of great importance in connection with the development of Brillouin integrated photonics and compact acousto-optical devices [4].

To increase the efficiency of stimulated Raman scattering (SRS) of light, we propose to use layered nanostructures of thin metal films with spatial dispersion and dielectric layers. Modeling the spatial dispersion of layered nanostructures consisting of thin metal films is also important in the context of the design of various metamaterials [5]. Spatial dispersion in a metal film arises due to the gas pressure of free electrons. The corresponding term (electron concentration gradient) is well known from the hydrodynamic equations in linearized form. The presence of spatial dispersion in the material leads to the appearance of additional spatial derivatives in the wave equation in nonlinear optics.

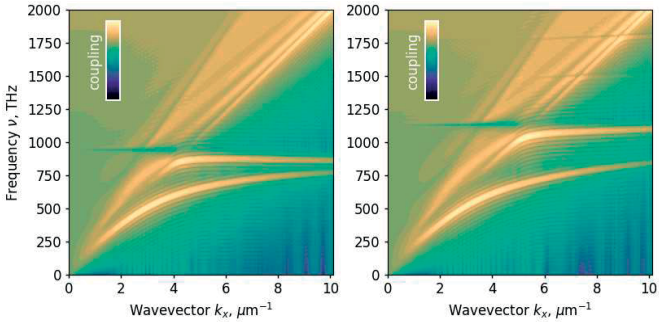

Fig. 1 Dispersion curves of a thin metal film 20 nm thick in the absence (left) and presence (right) of spatial dispersion. Material parameters: $\omega_p = 13.8 \cdot 10^{16}$ rad/s, $\varepsilon_\infty = 5.4$, $\tau = 40$ fs, $v_F = 3$ a.u.

Since existing packages for FDTD simulation do not have the ability to take into account the spatial dispersion of the material, we implemented this option in the code ourselves. Figure 1 shows the change in dispersion curves if the medium has this property. It can be seen that the frequency of zero permittivity (epsilon-near-zero, ENZ) increases when the material has spatial dispersion. Moreover, the magnitude of the displacement depends on the film thickness. The smaller the thickness, the greater the displacement. Another feature is the change in the slope of the dispersion curve corresponding to the high-frequency Ferrell-Berreman surface mode.

A simulation of SARS in a metal layer made of a material with spatial dispersion was carried out. The geometry of the problem was the same as in previous calculations - a flat metal layer between glass and air. The thickness of the layer varied. The source of incident monochromatic radiation in the two-dimensional TM problem was a linear magnetic dipole oriented perpendicular to the layer, and the moment of which is directed perpendicular to the simulation plane. In addition to the incident radiation, there was an artificial pumping of the phonon vibration in the volume of the metal layer, which played the role of interaction with the thermal bath, since the phonon vibration decays without this pumping. During the simulation, the amplitude of the resulting oscillation is analyzed.

As a result, it was possible to establish that if the Stokes radiation coincides with the ENZ frequency, then the amplitude of the phonon vibration becomes orders of magnitude higher than in the case of the anti-Stokes frequency hitting ENZ. However, both options have a larger phonon amplitude than in the absence of Raman scattering. In this case, the presence of spatial dispersion makes it possible to significantly reduce the phonon amplitude compared to the case of its absence. A possible mechanism for this effect is the interaction of Stokes and anti-Stokes waves, described above, which leads to inhibition of SRS. According to this explanation, spatial dispersion leads to spatial synchronism of all three waves. On the other hand, when incident radiation is below the ENZ frequency, the intensity of anti-Stokes radiation is always greater than the frequency of Stokes radiation, which suggests the possibility of implementing SARS amplified in a material with spatial dispersion.

The study was supported by the Russian Science Foundation No. 21-72-00052.

References

[1] J. Zhang, Q. Zhang, X. Wang, et al., " Resolved-sideband Raman cooling of an optical phonon in semiconductor materials," Nat. Photon. **10**, 600–606 (2016).

[2] M. Aspelmeyer, T.J. Kippenberg, F. Marquardt, " Cavity optomechanics," Rev. Mod. Phys. **86**, 1391–1452 (2014).

[3] A.R. Gazizov, M.Kh. Salakhov, S.S. Kharintsev, " Optomechanical heating and cooling via tip-enhanced Raman scattering in epsilon-near-zero medium," JETP Lett. **119**, 668-673 (2023).

[4] B.J. Eggleton, C.G. Poulton, P.T. Rakich, et al., " Brillouin integrated photonics," Nat. Photon. **13**, 664–677 (2019).

[5] L. Sun, Z. Li, T.S. Luk, et al., " Nonlocal effective medium analysis in symmetric metal-dielectric multilayer metamaterials," Phys. Rev. B. **91**, art.no. 195147 (2015).

Dielectric Particle Optimization: Kerker Effect by Evolution-inspired Algorithm

V. Igoshin[1], A. Kokhanovskiy[1], M. Petrov[1]*

[1]School of Physics and Engineering, ITMO University, Saint-Petersburg 197101, Russia

**e-mail address: m.petrov@metalab.ifmo.ru*

Recently, a new direction in photonics, called Mie-tronics, has emerged, enabling the creation of photonic devices with unique properties [1]. The dielectric particles are the building blocks of this new area. Therefore, further development of Mie-tronics necessitates the study of novel dielectric particle shapes and the effects that can be obtained in them. One of the effects that can be achieved in dielectric particles is the suppression of the backward-radiating field, known as the Kerker effect [2, 3]. The Kerker effect can be utilized to create devices that control light propagation direction and design dielectric antennas [3].

In this work, we investigate the scattering of electromagnetic waves on a dielectric structure constructed from N stacked cylinders of equal height with a refractive index $n = 4$. The incident plane wave of wavelength 600 nm propagates along the axis of the structure. The constraints are as follows: the height of the structure is bounded between 60 nm and 300 nm, and the radius of each cylinder ranges between 50 nm and 180 nm. The quantity characterizing the backward-radiating field is the backward radar cross-section:

$$\sigma_{RCS} = \lim_{r\to\infty} 4\pi r^2 \frac{|E_{bw}|^2}{|E_0|^2},$$

where $|E_{bw}|$ is the amplitude of field radiating in the backward direction, $|E_0|$ is the amplitude of the incident plane wave.

To design a structure with zero backward radiation, we employ the covariance matrix adaptation evolution strategy (CMA-ES) [4]. Examples of the optimized structures for $N = 1$, $N = 2$, and $N = 3$ are shown in Figure 1.

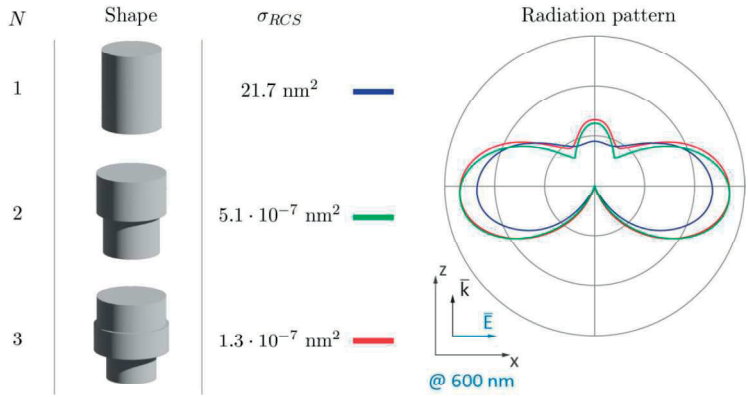

Fig. 1 Results of optimization for $N = 1$, $N = 2$, and $N = 3$ number of cylinders. The optimized shapes, backward radar cross-section values for each optimized shape, and radiation patterns are shown.

This work was performed with financial support of the Russian Science Foundation (Project No. 20-72-10141).

References

[1] Y. Kivshar, "The Rise of Mie-tronics," Nano Lett. **22**, 3513 (2022).

[2] A. Kuznetsov, et al., " Special scattering regimes for conical all-dielectric nanoparticles," Sci. Rep. **12**, 1 (2018).

[3] W. Liu, Y. Kivshar, "Generalized Kerker effects in nanophotonics and meta-optics [Invited]," Opt. Express, **26**, 13085 (2018).

[4] N. Hansen, A. Ostermeier, "Completely derandomized self-adaptation in evolution strategies," Evol. Comput., **9**, 159 (2001).

Effects of near-field interaction of luminescent $CeYTbF_3$ particles with colloidal nanoclusters of plasmonic nanoparticles

E. Izbasarova[1*], A. Gazizov[1]
[1]Kazan Federal University, Institute of Physics, 420008, Kazan, Russia
**e-mail address: Izbasarova.e.a@mail.ru*

Over the past few years, lanthanide doped luminescent nanoparticles (LNPs) have become promising materials due to their unique abilities to exhibit upconversion of photons [1] and thermal sensitivity [2]. In addition, the absence of both photobleaching and flashing give these nanoparticles special properties that make them ideal candidates for sensors and biological analyzers [3]. Many of these sensors utilize resonance energy transfer (RET) as a mechanism of action to detect a specific target molecule [4]. This is usually based on the transfer of energy from the excited state of the LNP (donor) to the ground state of a molecule or other material that acts as an acceptor, resulting in a change in the luminescence of the LNP. It has been demonstrated that plasmonic nanostructures placed in close proximity to LNPs are excellent tools for tuning the luminescence of upconversion by enhancing or quenching the luminescence intensity [5]. However, there are still some problems associated with the use of plasmon-enhanced upconversion, such as the low stability of some materials and possible damage to living cells at high light intensities [6]. Our ultimate goal is to develop a sensor to detect the presence of medically and biologically important molecules under aqueous solution conditions, keeping them alive and intact. This involves introducing nanoparticles into the solution to generate a signal without harming the molecules to be detected. During the interaction of gold nanoparticles with LNP, two competing effects arise: Förster near-field interaction and Purcell effect of a radiation enhancement in the far field. In order to enhance luminescence, it is important to avoid excessive energy consumption by gold, i.e., the predominance of the Förster effect. In this regard, our primary task is to determine the configurations and physical parameters in which the Purcell enhancement dominates over the Förster interaction.

For this purpose, we have simulated the dipole radiation amplification in LNP using the finite difference time domain (FDTD) method. We have carried out our study for various non-equivalent (by symmetry) configurations of up to 4 plasmonic nanoparticles (Au) surrounding LNP, as well as for LNP in nanoclusters located near the gold substrate. The total number of simulated configurations was 26, in 7 of which the nanocluster near the gold substrate was considered. As part of the research, a technique was developed that allows one to analyze the enhancement of the rates of radiative and non-radiative transitions, which opens up new prospects for increasing the sensitivity of sensors based on colloidal solutions of LNPs. One of the main findings of the work is the predominance of the Purcell enhancement effect over non-radiative losses due to Förster energy exchange at any distance between the 20-nm size LNP and the plasmonic nanoparticle of size 90 nm. In addition, the Purcell factor of all the simulated configuration was summed up in a detailed map of plasmonic enhancement Fig. 1.

Simulations show that the Purcell factor in the case of a single gold particle is about 100, and for clusters of two gold nanoparticles with the size considered in this work reach 300 at certain configurations and orientations of the dipole moment parallel to the dimer axis. When

a third and subsequent gold nanoparticle is added to the cluster, the value of the Purcell factor does not change significantly. Moreover, the probability of the formation of clusters with a large number of particles in a colloidal solution in the case when they do not stick together decreases with increasing number of particles. Nanoclusters with a large number of particles or located on a gold substrate support the excitation of plasmon resonance in other regions of the visible spectrum. Modeling of plasmon resonance in the presence of one or more analyte molecules near the LNP in a cluster of gold nanoparticles on a gold substrate leads to a small change in the spectral dependence of the Purcell factor, which allows to design a biosensor based on colloidal LNPs and plasmonic nanoparticles.

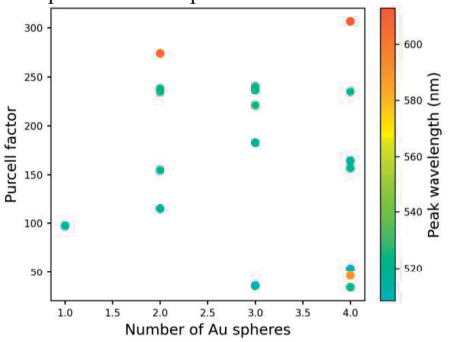

Fig. 1 The diagram showing the magnitude of Purcell factor for nanoclusters with different number of Au particles. The spectral position of plasmon resonance peaks is indicated by color.

These results made it possible to determine the optimal parameters and configurations of particle interaction for the creation of effective nanosensors based on either quenching or enhancing luminescence.

This work was financed by a subsidy allocated to the Kazan Federal University under the state assignment in the field of scientific activity (FZSM-2022-0021).

References

[1] X. Qin, J. Xu, Y. Wu, X. Liu, "Energy-transfer editing in lanthanide-activated upconversion nanocrystals: a toolbox for emerging applications," ACS Cent. Sci. **5**, 29-42 (2019).

[2] J.J. Talghader, M.L. Mah, E.G. Yukihara, and A.C. Coleman, "Thermoluminescent microparticle thermal history sensors," Microsyst. Nanoeng. **2**, 1-13 (2016).

[3] D. Mendez-Gonzalez, E. Lopez-Cabarcos, J. Rubio-Retama, M. Laurenti, "Sensors and bioassays powered by upconverting materials," Adv. Colloid Interface Sci. **249**, 66-87 (2017).

[4] Y. Han, M.O. Noor, A. Sedighi, U. Uddayasankar, S. Doughan, and U.J Krull, "Inorganic nanoparticles as donors in resonance energy transfer for solid-phase bioassays and biosensors," Langmuir. **33**, 12839-12858 (2017).

[5] D. Mendez-Gonzalez, S. Melle, O.G. Calderón, M. Laurenti, E. Cabrera-Granado, A. Egatz-Gómez, E. López-Cabarcos, J. Rubio-Retama, and J. Díaz, "Control of upconversion luminescence by gold nanoparticle size: from quenching to enhancement," Nanoscale. **11**, 13832-13844 (2019).

[6] D.M. Wu, A. García-Etxarri, A. Salleo, and J.A. Dionne, "Plasmon-enhanced upconversion," J. Phys. Chem. Lett. **5**, 4020-4031 (2014).

Luminescence temperature sensing based on spectral characteristic of CeF_3-TbF_3-YF_3 nanoparticles

S.I. Kalinichenko, A.S. Nizamutdinov, M.S. Pudovkin

Kazan Federal University, Institute of Physics, 18 Kremlyovskaya str, Kazan, 420008, Russian Federation

**e-mail address: delfinchik1290@gmail.com*

INTRODUCTION

Ratiometric luminescent thermometry is a non–contact temperature measurement technique based on the analysis of the luminescence spectral dependence on temperature. In this field, the Ce^{3+}/Tb^{3+} ion pair is considered very promising due to good separation between Ce^{3+} and Tb^{3+} peaks and phonon-assisted energy transfer character form Ce^{3+} to Tb^{3+}. Here we percent the temperature dependent spectral-kinetic characterization CeF_3-TbF_3-YF_3 nanoparticles and propose mechanism of temperature sensitivity.

MATERIALS AND METHODS

CeF_3-TbF_3-YF_3 nanosized samples were synthesized using co-precipitation method in water with subsequent microwave treatment. The excitation was performed via LOTIS TII tunable laser LT-2211A (λex (Ce^{3+}) = 266 nm, (pulse duration and repetition were 10 ns and 10 Hz, respectively). The spectra were detected via StellarNet (CCD) spectrometer. The kinetic characterizetion was carried out via monochromator connected with photomultiplier tube FEU-62 and digital oscilloscope Rhode&Schwartz with 1 GHz bandwidth.

RESULTS AND METHODS

Spectral and kinetic characterization of $Ce_{0.5}Y_{0.5-X}Tb_XF_3$ (X = 0.001, 0.002, 0.005, 0.01 and 0.05) nanoparticles was carried out in the temperature range of 303-523 K. To provide a deeper discussion of the temperature dependence of the spectra we took LIR of Ce^{3+} and Tb^{3+} luminescence peaks as a temperature-dependent parameter. The LIR functions decay with the temperature increase (Fig 1).

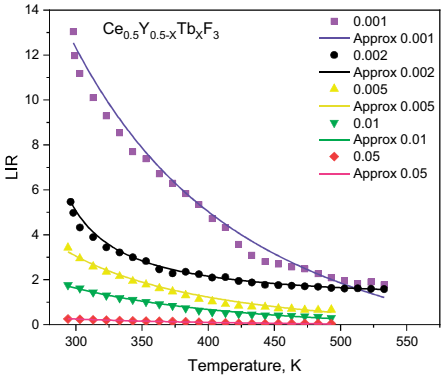

Fig. 1 The approximated LIR (ICe/ITb) dependences of Ce0.5Y0.5-XTbXF3 (X = 0.001, 0.002, 0.005, 0.01 and 0.05) nanoparticles.

Indeed, with the temperature rise, the depopulation rate of Ce^{3+} excited state by Tb^{3+} becomes higher (phonon-assisted process). Thus, the I_{Ce}/I_{Tb} decreases. However, the shape of the LIR decay decreases with the increase of Tb^{3+} concentration. It was suggested, that this phenomenon is related to the presence of two competing processes populating the $^5D_4$ state of Tb^{3+}. There are phonon-assisted non-radiate transition from $^5D_3$ to $^5D_4$ of Tb^{3+} and cross-relaxation between Tb^{3+} ions, which was considered less temperature dependent. The contribution of less temperature-dependent cross-relaxation. With the increase of Tb^{3+} concentration, the contribution of the less temperature dependent cross-relaxation process in the $^5D_4$ population leads to the decrease in the LIR descent rate. The luminescence decay time increases with the increase of temperature, probably due to above-mentioned cross-relaxation, that constantly populates the $^5D_4$ lever increasing the decay time (Fig 2) [1].

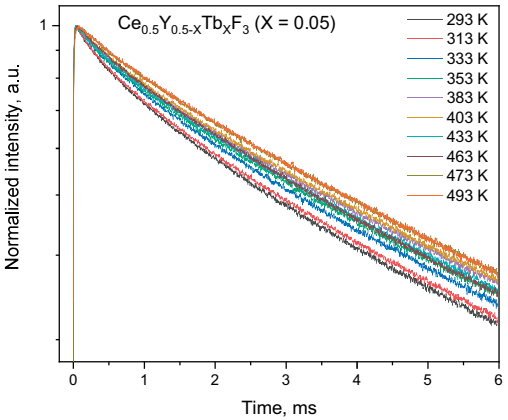

Fig. 2 Kinetics of luminescence decay in the 5D4 - 7F5 transitions of the Tb3+ ion in Ce0.5Y0.5-XTbXF3 nanoparticles (X = 0.05) detected in the temperature range 293 – 533 K.

References

[1] M. S. Pudovkin, S.I. Kalinichenko, A.S. Nizamutdinov, "CeF3-TbF3-YF3 nanoparticles for ratiometric temperature sensing" Optical Materials, vol. 148, January 2024

.

Mie-Resonant Lead-Free Halide Perovskite Particles for Up-Conversion Lasing and Second Harmonic Generation

D. Khmelevskaia[1,#*], S. Ilin[1,#], G. M. Maragkakis[2], S. Psilodimitrakopoulos[2], L. Mouchliadis[2], E. Stratakis[2], L. E. Zelenkov[1,3], S. V. Makarov[1,3]

[1]School of Physics and Engineering, ITMO University, Saint-Petersburg 197101, Russia

[2]Institute of Electronic Structure and Laser, Foundation for Research and Technology—Hellas, Heraklion, 71110 Crete, Greece

[3]Qingdao Innovation and Development Center of Harbin Engineering University, Qingdao 266404, China

[#]These authors contributed equally

**e-mail address: dariya.hmelevskaya@metalab.ifmo.ru*

Lead-free halide perovskites hold promise to become one of the most efficient family of environment-friendly materials for photonics and optoelectronics [1-2]. In particular, germanium-based halide perovskite attracts increasing attention as a promising non-toxic nonlinear material for up-conversion photonics [3-5]. Recently, germanium halide perovskites (in particular $CsGeI_3$) exhibit a strong second-order optical response with $\chi^{(2)}(2\omega;\omega,\omega) \approx 125$ pm/V exceeding that of many commercially available nonlinear optical materials (< 100 pm/V) and infrared (IR) excited photoluminescence. In this way, creation of optically resonant $CsGeI_3$ nanoparticles (NPs) is a prospective approach to further enhance second harmonic generation (SHG) and even achieve up-conversive laser generation. However, up-conversive laser generation in lead-free perovskites still has not been demonstrated yet, despite the fact that $CsGeI_3$ has relatively high refractive index ($n \approx 2.8$), and exciton binding energy of around $E_b = 16.7$ meV, and two-photon absorption coefficient ($\beta \approx 18.4$ cm/GW).

In this work, we develop a synthesis protocol to create $CsGeI_3$ NPs supporting Mie resonances that efficiently convert infrared light to visible both via lasing and SHG mechanisms. Such high-quality resonant NPs allow us to achieve up-conversion lasing in the broadband excitation wavelength (1200-1520 nm), which is accompanied by efficient spectrally tunable SHG with intensity comparable with that for lasing depending on temperature. This achievement becomes possible due to experimental and theoretical study of linear and nonlinear optical properties of $CsGeI_3$ material in the form of high-quality thin film and NPs of different sizes. Meanwhile, a significant one-order-of-magnitude enhancement of SHG was achieved in a single 480-nm NP through the coupling of incident light with a magnetic dipole resonance. Single-crystal character of individual $CsGeI_3$ NP is confirmed by careful study of polarization-resolved nonlinear optical imaging with high spatial resolution. In slightly larger particles, coupling of nonlinearly excited photoluminescence with higher-order optical modes has resulted in up-conversion lasing. This is the first demonstration of up-conversion lasing from lead-free perovskite. As a result, our study provides a novel strategy where individual NPs can support up-conversion lasing and SHG in a broad range of excitation wavelength.

We believe that our findings on simple and low-cost fabrication of $CsGeI_3$ optically resonant particles pave a new way for efficient, multifunctional, and environmentally friendly perovskite upconverters highly demanded in applications of nonlinear nanophotonics.

This research is supported by Priority 2030 Federal Academic Leadership Program.

References

[1] Fan, Qianqian, et al., "Lead-free halide perovskite nanocrystals: crystal structures, synthesis, stabilities, and optical properties," Angew. Chem. Int. Ed. **59**.3, 1030-1046 (2020).

[2] López-Fernández, Iago, et al., "Lead-Free Halide Perovskite Materials and Optoelectronic Devices: Progress and Prospective," Adv. Funct. Mater. **34**.6, 2307896 (2023).

[3] Stoumpos, Constantinos C., et al., "Hybrid germanium iodide perovskite semiconductors: active lone pairs, structural distortions, direct and indirect energy gaps, and strong nonlinear optical properties," J. Am. Chem. Soc. **137**.21, 6804-6819 (2015).

[4] Liu, Yang, et al., "Hybrid Germanium Bromide Perovskites with Tunable Second Harmonic Generation," Angew. Chem. Int. Ed. **61**.43, e202208875 (2022).

[5] Wang, Hebin, et al., "Chiral Hybrid Germanium (II) Halide with Strong Nonlinear Chiroptical Properties," Angew. Chem. Int. Ed. **62**.41, e202309600 (2023).

Modeling 3D Optical Trapping Of The Perovskite Particles

A. Kokhanovskiy[1], M. Vdovichenko[1], G. Romanenko[1], N. Kostina[1], Q. Song[1], I. Koryakina[1], M. Zyuzin[1], S. Makarov[1,2], M. Petrov[1]

[1]School of Physics and Engineering, ITMO University, Saint Petersburg 191002, Russia

[2]Qingdao Innovation and Development Center, Harbin Engineering University, Qingdao 266000, China

**e-mail address: gavriil.romanenko@metalab.ifmo.ru*

In this work, we numerically investigated the trapping of cubic perovskite particles ranging in size from 0.2 to 2.1 microns. We have detected a narrow region of optical particle trapping in three dimensions as the particle size changes. We have proposed a method for engineering the wavefront of the trapping beam to achieve stable particle trapping for all the size particles. Furthermore, we have proposed an experimental scheme of optical tweezers for trapping perovskite particles.

Perovskite particles are being used extensively in various applications such as optical chips, solar cells, UV photodetectors, and X-ray detectors. Resonant perovskite particles offer potential for creating integrated photonic devices with coherent radiation sources [1]. The synthesis of lead halide cubic-shaped particles has been achieved through methods like microfluidics [2] and hot injection [3].

The task of precisely positioning single sources on a metasurface can be solved using optical tweezers. However, the Gaussian profile of the trapping beam does not allow for stable trapping of particles of certain sizes.

The numerical calculation of the stiffness of the optical trap was implemented in the Optical Tweezers toolbox software environment. Figure 1 shows the stiffness of the optical trap in the plane of beam propagation depending on the particle size and refractive index (RI). Stable 3D trapping is observed only for a small range of the RI of particles near the RI of the medium. This explains the impossibility of controlling Perovskite particles $CrPbBr_3$ in three-dimensional space using the Gaussian profile of the trapping beam.

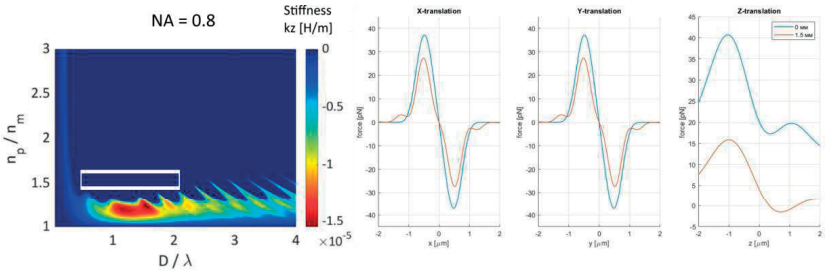

Figure 1 - Numerical calculation of the stiffness of an optical trap in the plane of propagation of the beam (a) depending on the particle size and the contrast of the refractive index of the medium and the particle. The wavelength of the trapping beam is 975 nm, the numerical aperture of the lens is 0.8. (b-d) The components of the optical force acting on the particle for the case of the Gaussian beam profile and the phase-modulated beam obtained by numerical simulation.

Optimization of the wavefront of the laser beam makes it possible to obtain a stable trapping of the particle (Figure 1 (b-d)). Figure 1 (b-c) shows the trapping force of an optical trap in a plane perpendicular to the propagation of the trapping beam for a Gaussian profile (blue line) and a centrally obstructed Gaussian beams (orange line). Figure 1 (d) shows the trapping force of an optical trap along the z-axis for a Gaussian beam and for a beam with a centrally

obstructed Gaussian beams. In the experiment, as an optimization of the wavefront, it can be carried out using a spatial light modulator (SLM). The SLM is integrated into the optical tweezer scheme, which allows you to dynamically control the wavefront of the laser beam. This, in turn, opens up the possibility of using machine learning algorithms to optimize the radiation wavefront.

In this work, we have shown the possibility of trapping cubic halogenide perovskite in three-dimensional space by modifying the wavefront of the trapping radiation. We also proposed an experimental method for modifying the wavefront using the spatial light modulator and machine learning algorithms.

The authors acknowledge financial support by the Russian Science Foundation (22-42-04420).

References

[1] Tiguntseva, E., Koshelev, K., Furasova, A., Tonkaev, P., Mikhailovskii, V., Ushakova, E. V., ... & Makarov, S. V., "Room-temperature lasing from Mie-resonant nonplasmonic nanoparticles," ACS nano, 14(7), 8149-8156, 2020

[2] Koryakina, I. G., Naumochkin, M., Markina, D. I., Khubezhov, S. A., Pushkarev, A. P., Evstrapov, A. A., ... & Zyuzin, M. V., "Single-Step Microfluidic Synthesis of Halide Perovskite Nanolasers in Suspension," Chemistry of Materials, 33(8), 2777-2784, 2021

[3] Parobek, D., Dong, Y., Qiao, T., & Son, D. H., "Direct hot-injection synthesis of Mn-doped CsPbBr3 nanocrystals," Chemistry of Materials, 30(9), 2939-2944, 2018

Synthesis and characteristics of luminescent probes for biological applications

Kokurina E. A, Mityushkin E.O., Leontiev A.V., Zharkov D.K., Shmelev A.G., Lyadov N.M., Nikiforov V.G.

Scientific adviser-assistant professor, PhD, Nikiforov V. G.

$NaYF_4$:Yb,Er upconversion nanoparticles were synthesized using a hydrothermal method. Replacing the cover with L-cysteine molecules made the nanoparticles hydrophilic and suitable for use in living objects. Upconversion nanoparticles (UCNPs) provide interesting opportunities for their using in a broad class of biological applications, such as biosensing[1], targeted drug delivery or bioimaging[2]. Among various types of phosphors, UCNPs based on fluoride crystals attract special attention, since they have excellent physicochemical stability and bright upconversion luminescence[3].

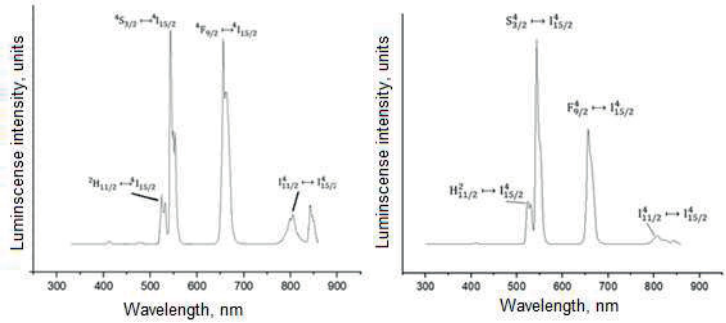

a) b)

Fig. 1. The spectrum of upconversion luminescence of nanoparticles a) before and b) after modification under laser excitation at wavelength of 980 nm.

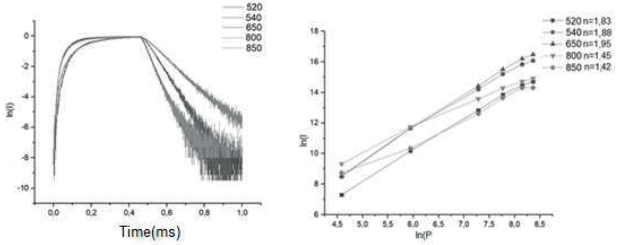

a) b)

Fig. 2. a)Normalized kinetics of luminescence of nanoparticles at wavelengths of 520, 540, 650, 800 and 850 nm under pulsed excitation at 980 nm with a duration of 0.5 ms. b) Dependence of luminescence intensity at wavelengths 520, 540, 650, 800 and 850 nm on laser power on a double logarithmic scale.

The thesis presents the results of the synthesis and characterization of nanoparticles with upconversion luminescence. To create biosensors, fluoride crystals with a $NaYF_4$ matrix are often chosen because of their low phonon energy (350 cm^{-1}), which minimizes energy losses for non-

radiative relaxation of lanthanides in intermediate excited states. $NaYF_4$:Yb,Er upconversion nanoparticles were obtained using a well-known hydrothermal synthesis method.

The hexagonal phase of the β-$NaYF_4$ crystal lattice largely determines the characteristic shape in the form of elongated rods with sizes of 60-80 nm × 1.2-1.5 μm. It is also important to note that nanoparticles can also have a cubic α-$NaYF_4$ phase with a different morphology[4]. In our case, the choice of a hexagonal structure is due to the presence of a crystal field, which promotes the radiative relaxation of rare earth ions, which significantly increases the quantum yield of luminescence. The synthesized UCNPs have an oleate shell, which gives them hydrophobic properties. To use UCNPs as bioprobes, their surface must be hydrophilic. For this purpose, the oleate shell is replaced with L-cysteine molecules ($C_3H_7NO_2S$). Note that the choice of the amino acid L-cysteine also provides the possibility of further modification of UCNP: the functional groups -NH_2, -COOH and -SH allow the attachment of various biomolecules to solve problems such as drug transport, bio-recognition, targeted delivery, phototherapy, etc.[5].

---

[1]Jiang W., Yi J., Li X, Niu N, He F, Chen L.: Biosensors. V.**12**, 1036 (2022).

[2]Rosal B., Jaque D.: Meth. Appl. Fluoresc. V.**7,** (2019)

[3]Art. No. 022001. 4. Li H., Tan M., Wang X.: J. Amer. Chem. Soc. V.**142,** 2023 (2020)

[4]Zou W.Q., Visser C., Maduro J.A., Pshenichnikov, M.S., Hummelen, J.C. Broadband: Nature Photonics. V.**6,** 560 (2012)

[5]Tu D., Liu Y., Zhu H.: Angew. Chem. Int. Ed. V.**125**, 1166 (2013).

PLASMON-ENHANCED FLUORESCENCE OF EGFP NEAR SILVER NANOCRESCENTS UPON ONE- AND TWO-PHOTON EXCITATION

Kudriavtseva S. Y, Bochenkov V. E.

M.V. Lomonosov Moscow State University, Moscow, Russia

e-mail address: owlsofya@gmail.com

Fluorescent proteins are an important tool of microbiology, in particular, for visualization of cellular structures and various processes in cells [1]. With the help of metal nanostructures and nanoassemblies of particles in which high-frequency localized charge oscillations are excited under the action of an electromagnetic wave, it is possible to significantly enhance the fluorescence intensity by increasing the excitation and emission rates, as well as the fluorescence quantum yield. This allows microscopic studies to be performed at lower excitation light intensities, which reduces negative effects on cells and increases the lifetime of fluorophores before photobleaching. The degree of fluorescence enhancement is determined by the dielectric properties of the metal and the size and shape of the nanoparticles. Advances in computational methods and techniques make it possible to predict and optimize the properties of nanostructures without the need to obtain them experimentally. The aim of this work was to study the fluorescence of green fluorescent protein near a crescent-shaped silver nanoparticle using the finite difference time domain (FDTD) method [2].

First, we calculated the extinction spectra of the crescent-shaped silver nanoparticle by varying the geometric parameters of the nanoparticle to achieve its best overlap with the EGFP spectrum. The spectrum of the selected particle has peaks near 500 and 950 nm, corresponding to the two modes of its electric field oscillations, which provides overlap with the emission band (510 nm) as well as with the single-(490 nm) and two-photon (950 nm) excitation bands of EGFP. For this particle, the electric field enhancement as the dipole modeling the protein moves away from its surface was calculated for single- and two-photon absorption: the highest excitation coefficients were observed at a distance of 3 nm from the particle and reached 19 and 1200, respectively. At the same points, the fluorescence quantum yields were predicted to be lowest (up to five orders of magnitude smaller) near the particle surface and increasing to 0.7 far away from the particle. As a result of modeling, it was found that in the presence of a crescent particle, the intensity of the radiative process increases by a factor of 17, and there appears a channel for the radiation-free transfer of excitation energy to the metal. The calculated radiative and non-radiative deactivation rate constants are $k_{fl} = 3{,}89 \cdot 10^{9}$ s^{-1} и $k_{loss} = 1{,}53 \cdot 10^{11}$ s^{-1} respectively, and the excited state lifetime is reduced to 6 ps.

References

1. Chudakov, D. M., Matz, M. V., Lukyanov, S., & Lukyanov, K. A. (2010). *Fluorescent Proteins and Their Applications in Imaging Living Cells and Tissues. Physiological Reviews, 90(3), 1103–1163.*
2. Allen Taflove, Computational Electromagnetics: The Finite-Difference Time-Domain Method. Boston: Artech House, (2005).

Нестационарные среды для аналоговых оптических вычислителей

В.М.Левковская[1*], А.В. Харитонов[1], С.С. Харинцев[1]
[1]Казанский федеральный университет, Казань, 420008, Россия
**e-mail address: levkovskaya.valeriya@gmail.com*

В последние годы наблюдается стремительный рост потребности в устройствах, способных быстро выполнять сложные ресурсоемкие вычисления. Вычислительная мощность классических цифровых компьютеров постепенно достигает своего предельного значения, что связано с физическими ограничениями на размер транзистора и рабочую частоту. В связи с этим необходимо искать альтернативные платформы для реализации суперкомпьютеров. В последнее время колоссальный интерес вызвали оптические аналоговые вычислители на основе метаматериалов [1]. В их основе лежит модуляция света – входящего сигнала – при его взаимодействии с пространственными неоднородностями. Выходящий сигнал (после взаимодействия) при должном дизайне метаматериала является результатом действия математического оператора на входящий сигнал. Было продемонстрировано, как экспериментально, так и теоретически, что с помощью вычислительных метаматериалов возможно решать интегро-дифференциальные уравнения и задачи оптимизации [2,3]. Благодаря тому, что вычисления проводятся по аналоговому принципу, скорость вычислений определяется лишь скоростью прохождения световой волны через оптическое устройство. Однако, для этой концепции требуются чрезвычайно сложные, зачастую нереалистичные, архитектуры метаматериала. К тому же малейшие неточности на этапе изготовления приводят к накоплению ошибок и неверному результату на выходе.

Целью настоящей работы является разработка физического механизма, позволяющего совершать аналоговые вычисления с помощью структур с простой геометрией. Для этого предложено использовать нестационарные оптические среды [4]. Под нестационарностью понимается быстрая, на масштабах меньших периода волны, модуляция показателя преломления. Идея разработанного принципа заключается в том, что модуляция показателя преломления происходит не в пространстве, а во времени, что дает фундаментально новую степень свободы в управлении электромагнитными полями. При быстром переключении среды возникает эффект временного отражения\преломления (time reflection/refraction). Суть эффекта заключается в том, что в сплошной среде при такой резкой модуляции возникает пара волн, движущихся в противоположных направлениях. В отличие от обычной пространственной границы, отраженная/преломленная во времени волна приобретает частоту, отличную от частоты падающего света, оставляя волновой вектор волны неизменным.

В представленной работе данный эффект заложен в принцип действия вычислительных оптических устройств. За счет дизайна временной неоднородности можно добиться нужной передаточной функции без внедрения сложной архитектуры. В результате работы были смоделированы передаточные функции при различных параметрах нестационарной среды. В качестве демонстрации была показана возможность реализации оператора дифференцирования второго порядка. Теоретические расчеты были подтверждены путем численного решения уравнений

Максвелла с помощью метода конечных разностей во временной области. Показано, что, меняя глубину модуляции, скорость модуляции и угол падения, можно получать четные передаточные функции. Причем изменение параметров модуляции можно совершать гибким образом, что позволит делать аналоговые устройства перепрограммируемыми. Последнее трудно реализуемо в стандартных вычислительных метаматериалах, так как требует дополнительной фабрикации. Также в работе изучено влияние дисперсии в среде с временной неоднородностью, а также скорости переключения показателя преломления.

Таким образом, был предложен новый механизм реализации оптических аналоговых вычислений, основанный на эффекте временного отражения/преломления света в нестационарных средах. Материалы с временной неоднородностью могут стать ключевым звеном на пути к полномасштабному внедрению аналоговых оптических суперкомпьютеров.

References

[1] Zangeneh-Nejad, F., Sounas, D. L., Alù, A., Fleury, R. "Analogue computing with metamaterials", Nat. Rev. Mater., **6**, 207-225 (2021).

[2] Silva, A., Monticone, F., Castaldi, G., Galdi, V., Alù, A., Engheta, N. "Performing mathematical operations with metamaterials", Science, **343**, 160-163 (2014).

[3] Mohammadi Estakhri, N., Edwards, B., Engheta, N. "Inverse-designed metastructures that solve equations", Science, **363**, 1333-1338. (2019).

[4] Galiffi, E., Tirole, R., Yin, S., Li, H., Vezzoli, S., Huidobro, P. A., Pendry, J. B. "Photonics of time-varying media", Adv. Photonics, **4**, 014002-014002. (2022).

CHIRAL PLASMONIC NANOCRESCENTS FOR SENSING: SYNTHESIS AND OPTICAL PROPERTIES

Lobanova E.M.[1], *Bochenkov V.E.*[1], *Bahratov I.A.*[2]

[1] Moscow State University, Chemical Department, Moscow, Russia
[2] Valiev Institute of Physics and Technology of Russian Academy of Sciences, Moscow, Russia
Postgraduate, Junior Researcher
katerina.m.lobanova@gmail.com

Nanomaterials based on plasmonic metal nanoparticles have great potential for medicine, pharmaceuticals and sensors. Their unique optical properties are due to the enhancement of local near fields under the influence of external electromagnetic waves upon the excitation of plasmon resonance. The optical properties of such nanomaterials depend on the characteristics of the nanoparticles: shape, size, material [1]. Therefore, the development of methods for the formation of new nanoparticles with a given shape is an urgent task. The plasmon resonance effect can be especially useful for studying the optical properties of chiral molecules, since they give very weak chiroptical signals due to the difference between molecular sizes and the wavelength of incident light [2]. One of the main methods for studying chiral molecules is circular dichroism spectroscopy (CD). It can be expected that in the field of chiral plasmonic nanoparticles, the CD signal of chiral molecules will also be enhanced.

The authors achieved the formation of chiral plasmonic silver nanocrescents using a combination of colloidal lithography and ion-plasma sputtering methods. The new technique makes it possible to obtain chiral nanocrescents of various orientations and widths by controlling the angles of deposition and sputtering (Scheme 1).

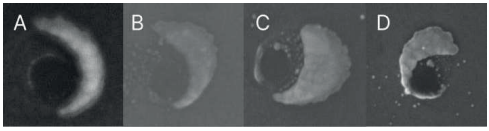

Scheme 1. SEM of chiral plasmonic nanocrescents of varying widths

It was shown that the resulting nanoparticles are characterized by enhanced absorption and a CD signal in the visible and near-IR region.

To sum up, a new formation method provides a rapid and inexpensive way of forming chiral nanocrescents. Along with the techniques commonly used to measure the optical properties of metal nanoparticles (extinction and fluorescence spectroscopy), we anticipate that CD will play an important role due to the number of effective ways it can be used to detect interactions between biomolecules and chiral plasmonic systems. Broader research is also needed to determine the relationship of crescent asymmetry with the CD signal and how to integrate such surfaces into functional commercial devices.

References

[1] Maier S.A. Plasmonics: Fundamentals and Applications / *New York, NY: Springer* **2007**
[2] Paiva-Marques W.A. et al. Chiral plasmonics and their potential for point-of-care biosensing applications // *Sensors (Switzerland). MDPI AG* **2020**. *20(3).* 944-963

Acknowledgements
This work was supported by the Russian Science Foundation (22-13-00126).

Chiral resonant waveguide design for reciprocal photon-electron transitions under extremely weak external magnetic field

N. G. Iukhtanov[1], I. A. Volkov[1], and M. V. Rybin[1,2]*
[1]*School of Physics and Engineering, ITMO University, Saint-Petersburg 197101, Russia*
[2]*Ioffe Institute, St Petersburg 194021, Russia*
**e-mail address: nikita.yuhtanov@metalab.ifmo.ru*

Abstract: Nanophotonic waveguides are crucial for controlling photon emission and scattering in modern photonic applications. By using chiral coupling in specialized designs, devices with polarization-dependent unidirectional light propagation can be created. Here we propose nanophotonic design with reciprocal photon-electron transition chiral coupling into waveguide volume subwavelength scale, enhancing light propagation control.

Introduction: Engineering photon manipulation devices is crucial in modern photonics, encompassing applications from light harvesting to quantum-information processing. Nanophotonic waveguides are favored for this purpose as they confine light, limiting its propagation directions. Chiral coupling in electron-photon systems is typically achieved in limited spaces using quantum dots or wells [1]. Detection schemes for light-matter interactions often necessitate ultra-high external magnetic fields to separate spin-dependent states by energy [2]. Cold atoms at very low temperatures also show promise for photonic applications [3, 4]. This study proposes a photonic waveguide design supporting transverse spin modes with both right-handed circular polarization (RHCP) and left-handed circular polarization (LHCP) within the waveguide volume. This design enables chiral coupling between photonic and electronic states using extremely weak external magnetic fields. The transition of spin-up excited electronic state to ground state emits RHCP photon through chiral coupling, while spin-down transition emits LHCP photon. This research investigates the chiral coupling between nanophotonic waveguide volume modes and electronic systems.

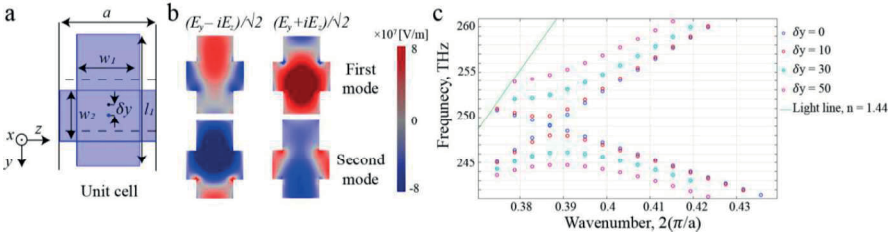

Fig. 1 (a) Schematic view of the realistic waveguide design unit cell, where δy is the shift along y-axis. The black dotted rectangle shows the centered position of the rectangular waveguide without breaking mirror symmetry. (b) Simulated mode circularity values for considering two modes ($x = 0$). (c) Simulated photonic band structure of the waveguide on the substrate (refractive index n is 1.44) with no external magnetic field.

The realistic chiral waveguide design: We propose a nanophotonic waveguide geometry supporting transverse spin modes and providing unidirectional characteristics for both considering modes. This waveguide design is realistic for fabrication process, which can be adapted as to silicon on insulator (SOI) as to gallium arsenide platform thanks to its

refractive index proximity in the near infrared frequency range. This design is shown on Figure 1a and contains a rectangular waveguide and transverse element (rectangular parallelepiped).

The waveguide (refractive index is 3.5) has thickness h = 440 nm (along x-axis), the waveguide period a = 450 nm, w_1 = 200 nm and w_2 = 160 nm are transverse element width and rectangular waveguide width, l_1 = 420 nm is the transverse element length. The broken mirror symmetry with δy shift produces a dominating volume polarization in either RHCP or LHCP for the waveguide (see Figure 1b). The typical anti-crossing behavior of mode branches is observed in this case (see Figure 1c). This effect is described in detail for the cases of magneto-induced non-reciprocity in silicon [5] and GaAs waveguides with averaged in-plane unidirectivity [6]. The simulation was performed with an eigenvalue solver of COMSOL Multiphysics. The waveguide geometry was optimized for the unidirectional propagation effect maximum considering the averaged volume of cube (100 nm^3) inside the center of the cross between the rectangular waveguide and transverse element. The maximum averaged directivity is approximately 92% at near to 245 THz for the first mode with δy = 50 nm, and −82% at near to 254 THz for the second mode with δy = 10 nm, where sign denotes the mode propagation direction.

Conclusion: To sum up, we have presented the device with chiral unidirectional propagation. In most cases, chiral coupling in an electron-photon system is realized with limited freedom degree and space by using quantum dots or wells. Here we have proposed the nanophotonic design with the possibility of reciprocal photon-electron transition with chiral coupling into the subwavelength scale of waveguide volume. The volume directivity, which is averaged by a cube of 100 nm^3 reaches more than 90% and 80% for the fabrication compatible nanophotonic waveguide for right- and left-hand polarized light, respectively. Furthermore, such waveguide provides the possibility of excited spin-dependent electron states spatial detection under extremely weak external magnetic field, which potentially reduces the costs of expensive cryogenic equipment in research laboratories.

Acknowledgement : This work was supported by Russian Science Foundation (23-72-10028).

References

[1] Lodahl, Peter, et al. "Chiral quantum optics", Nature, **541**, 7638, 473–480 (2017).

[2] Söllner, Immo, et al. "Deterministic photon–emitter coupling in chiral photonic circuits", Nature nanotechnology, **10**, 9, 775–778 (2015).

[3] Sayrin, Clément, et al. "Nanophotonic optical isolator controlled by the internal state of cold atoms", Physical Review X, **5**, 4, 041036 (2015).

[4] Mitsch, Rudolf, et al. "Quantum state-controlled directional spontaneous emission of photons into a nanophotonic waveguide", Nature communications, **5**,1, 5713 (2014).

[5] Iukhtanov, Nikita G., and Mikhail V. Rybin. "Resonant silicon waveguide with strong transverse electric field rotation for magnetic-field-induced non-reciprocity", Optics Letters, **48**, 11, 3043–3046 (2023).

[6] Volkov, Ilya A., and Roman S. Savelev. "Unidirectional coupling of a quantum emitter to a subwavelength grating waveguide with an engineered stationary inflection point", Physical Review B, **104**, 24, 245408 (2021).

Nonlinear Circular Dichroism in Achiral Nanostructures Irradiated by a Vortex Beam

***A. Nikitina*[1*] *and K. Frizyuk*[2]**

[1]*School of Physics and Engineering, ITMO University, Saint-Petersburg, 197101, Russia*

[2]*Department of Information Engineering, University of Brescia, Brescia, Italy*

**e-mail address: anastasia.nikitina@metalab.ifmo.ru*

Circular dichroism, which refers to the different responses of a material when exposed to the left- or right-circularly polarized light, is a well-known tool for exploring the properties of chiral molecules [1]. Over the past few years, this remarkable effect has been investigated in a wide range of systems, including second harmonic circular dichroism [2] or optical vortex dichroism [3] in chiral particles. In our recent work, we demonstrated that, along with chiral objects, even achiral ones can respond differently to the different polarizations of the incident field [4]. Specifically, we proved that the occurrence of circular dichroism in the second-harmonic signal in achiral nanostructures excited by a plane wave depends on the system's symmetry in an intricate way and follows a straightforward rule based on the relative position between the particle and the crystalline lattice of its material.

The aim of the current study is to reveal that, despite the simplicity of this rule, it can be applied to more complex systems: circular dichroism in higher-order harmonic generation in achiral nanostructures irradiated by a vortex beam (see Fig.1).

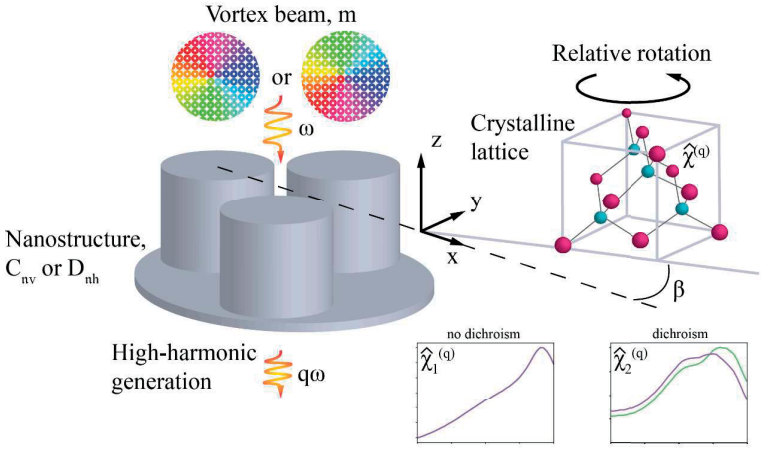

Fig. 1 Schematic of the concept. An achiral nanostructure, possessing symmetry C_{nv} or D_{nh}, is irradiated by an incident vortex beam with an angular momentum projection of $\pm m$ on the z-axis, dependent on its handedness. This

generates a high-harmonic of order q. The crystalline lattice of the material, characterized by the nonlinear susceptibility tensor $\hat{\chi}^{(q)}$ is rotated with respect to the sample about the z-axis by an angle β. The occurrence of nonlinear circular dichroism in this system depends on the both the symmetry of the nanostructure and the crystalline lattice, as well as their relative position, but is independent of the order of high-harmonic and the incident vortex beam.

In particular, we consider an achiral nanostructure whose rotational symmetry is described by the number n, and which is made from a material with a noncentrosymmetric crystalline lattice capable of producing high-harmonic generation. A high-harmonic of order q is excited in this sample by the incident vortex beam which has an angular momentum projection $\pm m$ on the z-axis, depending on its handedness. The crystalline lattice of the material is characterized by the nonlinear susceptibility tensor $\hat{\chi}^{(q)}$, which can be expressed in the cylindrical coordinates, comprising several terms that differ by momentum projection m_χ.

We define high-order nonlinear circular dichroism as the difference between the total integral intensities of a high-harmonic under left- or right-handed beam irradiation. By introducing Δm as the difference between different projections m_χ, we present an elegant rule to determine the possibility of this nonlinear effect: if Δm_χ can be equal to $n\nu$, where $\nu \in \mathbb{Z}$, then high-harmonic circular dichroism can appear, but only under certain conditions. Specifically, it can be observed only if the crystalline lattice is rotated with respect to the sample about the z-axis by angle $\beta \neq \pi\nu/\Delta m_\chi$.

Thus, we show the independence of the conditions for the appearance of nonlinear circular dichroism in achiral nanostructures, as previously estimated [4], from the order of high-harmonic generation and the vortex beam. Our study not only verifies the surprising result that allows for quickly determining the possibility of this widely applicable nonlinear effect, but also offers a detailed theoretical framework for obtaining conditions for other systems.

This work was performed with financial support of the Russian Science Foundation (Project No. № 22-12-00204).

References

[1] N. J. Greenfield, "Using circular dichroism spectra to estimate protein secondary structure, "Nat. Protoc., 1, 2876–2890 (2006).

[2] F. Spreyer, J. Mun, H. Kim, R. M. Kim, K. T. Nam, J. Rho, and T. Zentgraf, "Second Harmonic Optical Circular Dichroism of Plasmonic Chiral Helicoid-III Nanoparticles," ACS Photonics, 9(3), 784–792 (2022).

[3] K. A. Forbes and G. A. Jones, "Optical vortex dichroism in chiral particles," Phys. Rev. A, 103(5), 053515 (2021).

[4] A. Nikitina, A. Nikolaeva, and K. Frizyuk, "Nonlinear circular dichroism in achiral dielectric nanoparticles," Phys. Rev. B, 107(4), L041405 (2023).

Engineering the radiative lifetime of excitons in two-dimensional van der Waals heterostructures

P. Pantyukhina[1*], A. Bogdanov[2], K. Koshelev[3]

[1] School of Physics and Engineering, ITMO University, Saint-Petersburg 197101, Russia

[2] Harbin Engineering University, Qingdao Innovation and Development Center, Qingdao, Shandong, China

[3] Nonlinear Physics Center, Research School of Physics, Australian National University, ACT 2612, Australia

**e-mail address: polina.pantuhina@metalab.ifmo.ru*

Excitons are crucial for the optical properties of heterostructures with quantum wells (QW). Recent advancements in fabricating nanoscale van der Waals (vdW) heterostructures, including ultra-thin semiconductors and monolayer transition metal dichalcogenides (TMD), have enabled the domination of optical transitions by spontaneous emission mechanisms [1]. Integrating a two-dimensional semiconductor layer into a photonic structure activates the interaction between excitons and photon modes, modifying the local density of optical states. Recent work shows a significant increase in the speed of spontaneous emission of excitons through the integration of TMD monolayers with resonant photonic structures [2]. The reverse effect, suppression of spontaneous emission using nano-structured optical resonators, is of interest for understanding the dynamics of excitons.

In this study, we investigate the increase in radiative lifetime of excitons in two-dimensional TMD monolayers integrated with dielectric photonic structures. Key results include the development of an analytical model describing weak coupling between excitons and leaking modes of a dielectric waveguide, identifying conditions for maximizing exciton radiative lifetime enhancement, which reaches n^2, where n is the refractive index of the waveguide material. As well as numerical analysis of a periodic photonic structure with an integrated QW. In this case, the reduction in exciton radiation losses can be many orders of magnitude greater than in the case of a waveguide due to the complex structure of resonances and optical states. The theory developed can be applied to devise methods for controlling and manipulating exciton properties in two-dimensional vdW heterostructures for various applications. The developed theory explains and expands the results of recent experiments [3].

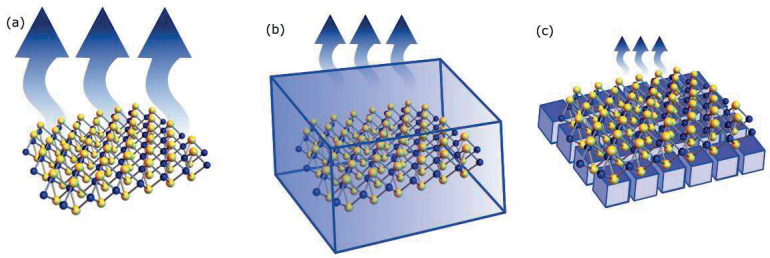

Fig. 1 (a) Spontaneous emission of excitons in a TMD located in vacuum; (b) Reduction of spontaneous emission of excitons in the case when the TMD is in a plane-parallel dielectric waveguide; (c) Greater suppression of spontaneous emission of excitons in the case when the TMD is combined with a metasurface. TMD image adapted from [4].

Acknowledgment

This work was performed with financial support of the Russian Science Foundation (Project No.21-72-30018).

References

[1] F. Cadiz, et al. "Excitonic linewidth approaching the homogeneous limit in MoS 2-based van der Waals heterostructures." Physical Review X, **7**(2), 021026 (2017).

[2] Y. C. Lee, Y. C. Tseng, and H. L. Chen, "Single type of nanocavity structure enhances light outcouplings from various two-dimensional materials by over 100-fold." ACS photonics, **4**(1), 93-105, (2017).

[3] H. H. Fang, et al. "Control of the exciton radiative lifetime in van der Waals heterostructures." Physical review letters, **123**(6), 067401, (2019).

[4] M. Szyniszewski, *Low-dimensional quantum system,* (Lancaster University, United Kingdom, 2016).

Vortex polarization of bound states in the continuum in luminescence response of 2D-photonic crystals with Ge(Si) nanoislands

A. Peretokin[1*], M. Stepikhova[1], D. Yurasov[1], M. Shaleev[1], D. Shengurov[1], S. Dyakov[2], Zh. Smagina[3], E. Rodyakina[3,4], A. Novikov[1,5]

[1] Institute for Physics of Microstructures Russian Academy of Sciences, GSP-105, Nizhny Novgorod, 603950, Russia

[2] Skolkovo Institute of Science and Technology, Bolshoy Boulevard 30, bd. 1, Moscow, 121205, Russian Federation, Moscow, Russia

[3] Rzhanov Institute of Semiconductor Physics, Siberian Branch of Russian Academy of Sciences, 13 Lavrentiev aven., Novosibirsk, 630090, Russia

[4] Novosibirsk State University, 1, Pirogova str., Novosibirsk, 630090, Russia

[5] Lobachevsky State University of Nizhny Novgorod, 23 Gagarin Avenue, 603950 Nizhny Novgorod, Russia

**e-mail address: aperetokin@ipmras.ru*

Currently, bound states in the continuum (BICs) attract a lot of attention from the scientific community. As is well known, BICs are waves that remain localized even though they coexist with a continuous spectrum of radiating waves that can carry energy away. BICs can exist in many types of photonic systems, and, as has been shown theoretically and experimentally, they exist in 2D photonic crystal slabs (PhCs) [1,2]. BICs localized at the Γ-point of the reciprocal space are usually called "symmetry-protected" because of their symmetry incompatibility with the continuum. One can also describe this phenomenon from a topological point of view. In article [3], the authors demonstrated that the BiCs are vortex centres in the polarization directions of far-field radiation, which are characterized by a topological charge q. The charge q shows how many times the polarization vector winds around the BIC.

In this paper, we will show for the first time the vortex structure of polarization in the far field associated with various PhC modes, based on photoluminescence measurements. PhCs with a hexagonal lattice corresponding to C6v symmetry were studied. Measurements of their photoluminescence response allowed us to directly observe the rotation of the polarization vector of PhC modes when bypassing the Γ-point in momentum space. We show that the topological charge q is different for different PhC modes. So, for singlet mode A_2 $q = +1$, but for doublet modes E_2 $q = -2$. As far as we know, these are the first results of topological charge studies performed for different modes of PhC.

To show this, we used an original technique of photoluminescence measurements with angular resolution. This technique allows measurements in momentum space. The measurements were carried out in mirco-photoluminescence (micro-PL) setup, in which a diaphragm introduced into a parallel beam formed by the objective provided the angular resolution. The center of the parallel beam corresponds to the Γ-point in momentum space. Diaphragm displacement in relation to the selected symmetry direction of the Brillouin zone makes it possible to experimentally measure the features of PhC band structure in the far field [4]. For polarization measurements, a polarizer was added into the parallel beam after

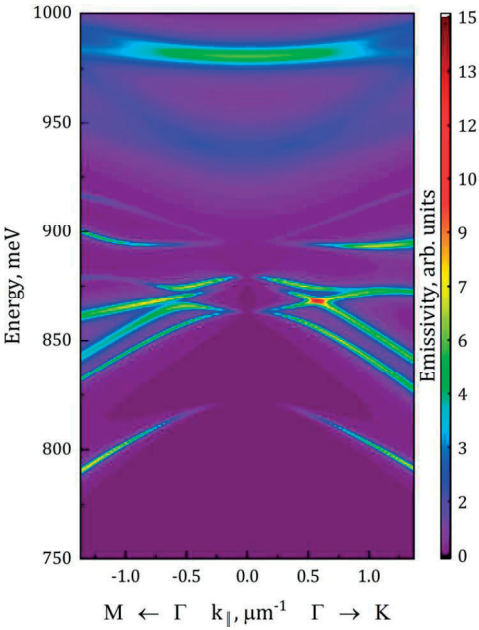

Fig 1 – The band structure of the photonic crystal, the color shows the emissivity.

diaphragm. Moving away from the Γ-point, photoluminescence spectra were measured for different rotation angles of the polarizer, then, according to the measurement data, the polarization of each mode at a selected point in the momentum space was determined. For these studies, we used PhCs with embedded Ge(Si) nanoislands. Structures of this type were grown on SOI substrates.

For study, a photonic crystal with a hexagonal lattice of holes was chosen, with the following parameters: total thickness of the Si layer $h_{Si} = 335$ nm, etching depth of the holes $h_{etch} = 250$ nm, lattice period $a = 575$ nm and hole radius $r = 0.25a$. The results of numerical simulation of the band structure of this PhC are shown at figure 1. All measurements were carried out at room temperature. The structures under discussion are of interest from the point of view of their possible applications, in particular, for creating compact near-IR sources compatible with silicon technologies.

Foundation

The work was supported by FASO, project #FFUF-2024-0019.

References

[1] C.W. Hsu, B. Zhen, A.D. Stone, J.D. Joannopoulos, and M Soljačić, "Bound states in the continuum", Nature Reviews Materials **1**, 16084 (2016).

[2] S.A. Dyakov, M.V. Stepikhova, A.A. Bogdanov, A.V. Novikov, D.V. Yurasov, M.V. Shaleev, Z.F. Krasilnik, S.G. Tikhodeev, N.A. Gippius, "Photonic Bound States in the Continuum in Si Structures with the Self-Assembled Ge Nanoislands", Laser and Photonics Rev. **15**, 2000242 (2021).

[3] B. Zhen, C.W. Hsu, L. Lu A.D. Stone, and M Soljačić "Topological Nature of Optical Bound States in the Continuum", Phys. Rev. Lett. **113**, 257401 (2014).

[4] A.V. Peretokin, D.V. Yurasov, M.V. Stepikhova, M.V. Shaleev, A.N. Yablonskiy, D.V. Shengurov, S.A. Dyakov, E.E. Rodyakina, Zh.V. Smagina, and A.V. Novikov "Tuning the Luminescence Response of an Air-Hole Photonic Crystal Slab Using Etching Depth Variation", Nanomaretials **13**, 1678 (2023).

Enhancement of Linear and Nonlinear Optical Effects in Single-Walled Nanotubes through Interaction with Bound States in the Continuum

A. Seredin

School of Physics and Engineering ITMO University, Saint-Petersburg 197101, Russia

e-mail : Albert.seredin@metalab.ifmo.ru

In the realm of quantum photonics, quantum cryptography, quantum computing, and the broader field of quantum optics research, the significance of single photon sources cannot be understated. The development and utilization of single photon sources are essential for advancements in these areas. Scientists have achieved notable progress in acquiring single photon sources through various techniques, including quantum dots [1], defect centers in crystals [2], semiconductor nanowires [3], superconductors [4], and doped single-walled carbon semiconductor nanotubes (SWNTs) operable at room temperatures [5]. Among these techniques, SWCNTs stand out due to their unique ability to control chirality parameters, allowing for precise spectral control over the exciton transition's position [6]. However, SWCNTs are hindered by their comparatively lower quantum yield (10-30%) compared to other emitter options [7].

Efforts to improve the quantum yield of photons from individual sources necessitate a comprehensive approach that considers both the fine-tuning of source characteristics and the design platforms employed. By integrating SWCNTs with nanostructures, adjustments can be made to the radiative and non-radiative lifetime of photons, ultimately leading to an enhanced quantum yield in the final device [8].

In the context of optical resonances within single nanostructures, the role of collective effects that emerge from organizing such structures into one-dimensional chains and two-dimensional metasurfaces is fundamental. The creation of these arrays results in a substantial increase in the quality factor of existing resonances, facilitating the exploration of phenomena specific to collective effects.

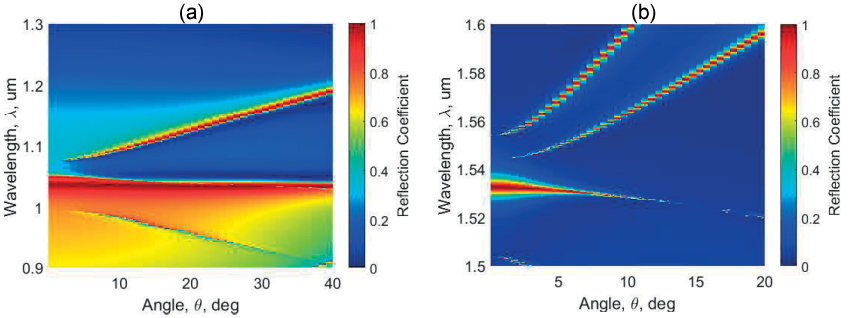

Fig. 1 TM polarization reflectance map for silicon photonic crystal (a) double resonance for single photon emission in functionalized SWNTs, (b) triple resonance for spontaneous FWM in SWNTs film

An example of a notable collective effect observed in metasurfaces is the presence of bound states in the continuum (BIC) [9]. The distinctive features of such collective resonances hold great potential for the advancement of integrated nanophotonics and quantum cryptography, particularly in the near and mid-infrared range, with implications for telecommunications applications.

This study aims to explore two distinct cases concerning the optical properties of nanotubes. Firstly, we investigate the enhancement of photon emission in functionalized SWNTs within the linear regime. Secondly, we delve into the generation of photon pairs through spontaneous four-wave mixing in SWNTs under the nonlinear regime.

Linear Regime: The reflectance map in fig. 1 (a) illustrates the spectral coverage of resonances for a silicon photonic crystal. By adjusting certain configurations, BIC modes can be specifically tuned to align with the pump and photoluminescence wavelengths of individual functionalized nanotubes, in this way we achieve double resonance matching.

Nonlinear Regime: Single-Walled Nanotubes (SWNTs) exhibit a non-zero third order susceptibility [10], providing potential for developing a device capable of generating entangled photon pairs. To optimize the efficiency of photon pair generation through spontaneous four-wave mixing, a solution is proposed in the form of a triple BIC resonance (fig. 1 (b), comprising 2 BIC resonances at the gamma point and 1 BIC parametric resonance). Through careful arrangement of these branches, the process of four-wave mixing can be facilitated at certain angles and pump wavelengths, ensuring equidistant energy distances and compliance with the law of conservation of wave vectors.

References

[1] Michler, Peter, et al. "A quantum dot single-photon turnstile device," science **5500**, 2282-2285 (2000).

[2] Aharonovich, Igor, Dirk Englund, and Milos Toth. "Solid-state single-photon emitters," Nature photonics **10**, 631-641 (2016).

[3] Claudon, Julien, et al. "A highly efficient single-photon source based on a quantum dot in a photonic nanowire," Nature Photonics **3**, 174-177 (2010)

[4] Natarajan, Chandra M., Michael G. Tanner, and Robert H. Hadfield. "Superconducting nanowire single-photon detectors: physics and applications," Superconductor science and technology **6,** 063001 (2012)

[5] He, Xiaowei, et al. "Tunable room-temperature single-photon emission at telecom wavelengths from sp 3 defects in carbon nanotubes," Nature Photonics **9**, 577-582 (2017)

[6] Bachilo, Sergei M., et al. "Structure-assigned optical spectra of single-walled carbon nanotubes," science **5602,** 2361-2366 (2002)

[7] Ghosh, Saunab, et al. "Oxygen doping modifies near-infrared band gaps in fluorescent single-walled carbon nanotubes," Science **6011,** 1656-1659 (2010)

[8] He, X., et al. "Carbon nanotubes as emerging quantum-light sources," Nature materials **8,** 663-670 (2018)

[9] Hsu, Chia Wei, et al. "Bound states in the continuum," Nature Reviews Materials **9**, 1-13 (2016)

[10] Nemilentsau, A. M., et al. "Third-order optical nonlinearity in single-wall carbon nanotubes." Carbon **11**, 2246-2253 (2006)

Simulation of the optical vortices observed in liquid crystals using Jones matrix formalism

***A. Shalev*[1*], *I. Lobanov*[1]**
[1]*School of Physics and Engineering, ITMO University, Saint Petersburg, Russia*
**e-mail address: artem.shalev@metalab.ifmo.ru*

Modern optics and photonics require innovative materials and solutions to create miniature and efficient optical devices. Diffractive optical elements (DOEs) are flat optical components that manipulate light waves by modulating their amplitude or phase. DOEs have subwavelength or near-wavelength structures, which make them useful for creating high-quality images and other applications [1-3]. However, there are several challenges to commercializing DOEs. One major obstacle is their sensitivity to changes in wavelength and environmental factors, such as temperature and humidity. These factors can significantly affect the performance of the DOEs and the quality of the images they produce. To address this challenge, researchers are exploring the development of dynamic DOEs that can adapt to different environmental conditions and tasks. One promising approach is using liquid crystals, which can be manipulated to change the properties of the DOE [4-6]. This could lead to more versatile and efficient optical components for various applications.

The scientific problem of creating and studying the properties of optically anisotropic, topologically structured liquid crystals for developing optical and photonic systems is at the intersection of research fields in condensed matter physics, optical physics, and photonics. In the context of research on localized liquid crystal structures, two main areas of scientific activity can be identified: 1) the actual creation of complex, localized orientational states in liquid crystals and the investigation of their internal structural organization; and 2) the investigation of optical and photonic characteristics of localized liquid crystalline structures. Within liquid crystals (LC), there is a characteristic alignment of dipole molecules along a specific direction, determined by a single vector known as the «director». In this work, we generate the director field using the approach described in publication [7] and study its optical properties using modeling based on the Jones matrix formalism.

The Jones vector describes the polarization of light in a vacuum or other homogeneous and isotropic medium, in the absence of absorption. In such a medium, light can be represented by a transverse electromagnetic wave, and to study polarization it is sufficient to know only the polarization of the electric field. While the Jones vector represents an arbitrary field polarization (linear, circular, elliptical), the Jones matrix represents an optical element, such as a polarizer or anisotropic medium with an arbitrary thickness. Therefore, the Jones matrix formalism allows us to numerically investigate the optical properties of liquid crystals.

In this work, we theoretically calculate the director field of liquid crystal using approach from [7], then we construct an optical scheme (Fig.1a), where circular polarized field irradiate the sample, then polarization of the field from the sample is transformed to linear and combined with linear polarized at specific transmission angle. Amplitude (Fig.1b) and phase (Fig.1c) were calculated from the output Jones vectors.

On the phase distribution of the electric field 2π phase foray is observed. This indicates the presence of an optical vortex with a topological charge $q=2$.

Both calculated amplitude and phase results are in a good coincidence with an experiment.

This work was performed with financial support of the Russian Science Foundation № 23-72-10028.

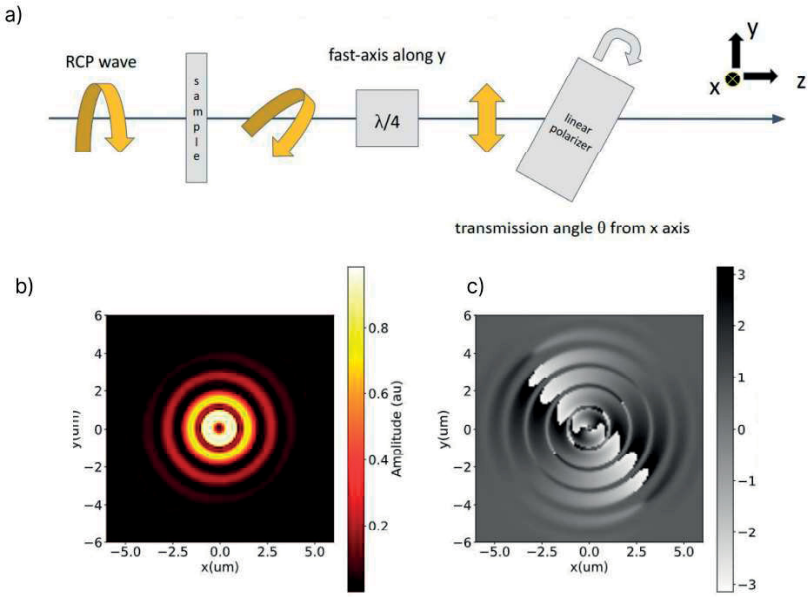

Fig. 1 a) optical scheme used in a model, each optical elements has its own Jones matrix representation; b) amplitude and c) phase distribution of the electric field after the linear polarizer with transmission angle θ=45°

References

[1] Bhattacharya S. Simplified mesh techniques for design of beam-shaping diffractive optical elements. Optik, 2008, 119(7): 321-328.

[2] Liu S, Liu C Y, Jin G, et al. Design of an omnidirectional gaze optical imaging system with ultrahigh resolution. Optical Review, 2021, 28(1): 8-17.

[3] Yang S P, Kim J B, Seo Y H, et al. Rotational offset microlens arrays for highly efficient structured pattern projection. Advanced Optical Materials, 2020, 8(16): 2000395.

[4] Stalder M, Ehbets P. Electrically switchable diffractive optical element for image processing. Optics Letters, 1994, 19(1): 1-3.

[5] Lou Y M, Liu Q K, Wang H, et al. Rapid fabrication of an electrically switchable liquid crystal Fresnel zone lens. Applied Optics, 2010, 49(26): 4995-5000.

[6] Kobashi J, Yoshida H, Ozaki M. Planar optics with patterned chiral liquid crystals. Nature Photonics, 2016, 10(6): 389-392.

[7] Lobanov, I.; Aksenova, E.; Orlova, T.; Darmoroz, D.; Uzdin, V.; Kiselev, A.D. Optical Imaging and Analytical Design of Localized Topological Structures in Chiral Liquid Crystals. *Symmetry* 2022, *14*, 2476. https://doi.org/10.3390/sym14122476

REFORMULATED FOURIER MODAL METHOD WITH ANALYTICAL TREATMENT OF THE FIELD DISCONTINUITIES AND ADAPTIVE SPACE RESOLUTION

S. Spiridonov[1*], A. Scherbakov[2]

[1,2]School of Physics and Engineering, ITMO University, Saint-Petersburg 197101, Russia

**e-mail address: sergey.spiridonov@metalab.ifmo.ru*

In our work, we have developed a novel formulation of the Fourier modal method (FMM) for solving diffraction problems in two-dimensional, periodic structures. This new approach explicitly considers the boundary conditions of discontinuous components of the electric field and leads to a set of matrix equations that avoid the need for matrix inversion. Furthermore, we have also proposed additional enhancements to this approach by including the adaptive spatial resolution approach.

The Fourier modal method has gained great popularity due to its versatility and relative ease of implementation [1]. This method is well-suited for solving diffraction and scattering problems on periodic metallic and dielectric structures, modeling solar cells, and nonlinear optics problems. The idea of the method is to solve Maxwell's equations in a truncated Fourier space using Bloch's theorem. The system of differential equations is reduced to an eigenvalue problem, within which it is necessary to reverse the matrix of the Fourier components of the permittivity. Next, the transfer matrix and scattering matrix approaches are used to determine diffraction orders. This technique has been significantly enhanced through the application of factorization methods for discontinuous functions in the Fourier space, commonly referred to as Li factorization rules [2]. However, despite this, the main disadvantages of the method remain the Gibbs effect, which implicitly affects convergence and distorts the calculation of the near field, and the need to solve the matrix-vector eigenvalue problem at one of the stages of the method which is computationally challenging.

In our work, we present a new formulation of the Fourier modal method with analytical treatment of the field discontinuities. The key idea behind this approach is to separately consider and take into account the boundary conditions of the discontinuous and continuous components of the electric field. This leads to new matrix equations in the old plane wave basis, in which it is not necessary to reverse the permittivity matrix. This approach has been previously tested by the authors in the simplest one-dimensional case, as described in their paper [3]. The key benefits of the new approach are a significantly more accurate calculation of the near-field within the structure, and the elimination of the need for inverting the permittivity matrix. This work presents a new formulation and numerical validation for the case of two-dimensional lattice structures.

In addition, this paper also presents a further improvement of the developed formulation by combining it with the adapted spatial resolution approach [4]. The resulting formulation retained the advantages of both approaches.

The developed new formulations have the potential to form the basis for more efficient methods, such as those based on matrix perturbation theory for solving eigenvalue problems, and could be applied to a variety of problems in numerical modeling of nanoscale periodic structures.

Acknowledgments

The first part of the work, the development of a new formulation for the two-dimensional case, was supported by the Russian Science Foundation, grant No. 22-11-00153.

The second part of the work, the development of the new formulation through the use of an adapted spatial resolution approach was supported by the ITMO-MIPT-Skoltech Clover Program.

References

[1] M. G. Moharam, E. B. Grann, D. A. Pommet, and T. K. Gaylord, "Formulation for stable and efficient implementation of the rigorous coupled-wave analysis of binary gratings," Journal of the Optical Society of America A, vol. 12, pp. 1068–1076, 5 May 1995

[2] L. Li, "Use of fourier series in the analysis of discontinuous periodic structures," JOSA A, vol. 13, no. 9, pp. 1870–1876, 1996.

[3] Spiridonov S., Shcherbakov A. A. Reformulated Fourier Modal Method with improved near field computations //Journal of Computational Science. – 2023. – Т. 67. – С. 101936.

[4] Granet G. Reformulation of the lamellar grating problem through the concept of adaptive spatial resolution //JOSA A. – 1999. – Т. 16. – №. 10. – С. 2510-2516.

Scanning probe instrumentation providing tip-enhancement effects in photoluminescence and Raman spectra micro-scale mapping

1Limited Liability Company "ACTIVE PHOTONICS", Moscow, Zelenograd, Russia

Dr. M.A.Trusov et al.

NT-MDT Group

NT-MDT company brand is well-known all over the world as one of the market and technology leaders providing the equipment to work in nano-scale surface research and spectral research. We have a long story in this business. In particular, we were the first team who suggested for the scientific research the SPM+Raman+PL combined instrument, allowed to measure the optical properties of a sample surface with nanometer spatial resolution.

That case had happened more than 20 year ago, and we have been developing strongly our technologies from that time. For now, we are presenting a new-generation SPM+Raman+PL equipment with a very flexible design, yielding many possibilities to realize cumbersome experiments in probe nanoscopy and optical spectroscopy.

On the Workshop we are going to present our basic approach on designing multi-mode confocal micro-spectrometers, and their combinations with SPM/AFM , and would like to show some preliminary but promising results obtained on our instruments. Also, we will talk on possible extension of the experimental techniques in a scope of multi-photon experiments and study of non-linear interaction between light and probe. An essential part of a set of techniques realized on our instruments is the tip-enhanced Raman scattering (TERS) and the tip-enhanced photoluminescence (TEPL) measurement modes; and we'll talk about it too.

To provide for the experimentalists the full solution for nano-optical measurements, our team is strongly elaborating now the Raman and PL laser design and production, and these lasers are already successfully exploited in scientific laboratories. They provide high-quality beams, good stability, and have got a long life-time. In addition, we had started recently a new project on manufacturing scientific-grade CCD spectral detectors; this subject also will be touched in our talk.

Subradiant states in planar arrays of dipolar emitters

I. Volkov, N. Ustimenko, D. Kornovan, S. Mitsai, S. Zhogolev, A. Sheremet, R. Savelev, Mihail Petrov

[1]*School of Physics and Engineering, ITMO University, Saint-Petersburg 197101, Russia*

**e-mail address: r.savelev@metalab.ifmo.ru*

The optically trapped ensembles of cold atoms provide a versatile platform for storing and coherent manipulation of quantum information. However, efficient realization of quantum information processing requires long-lived quantum states protected from the decoherence e.g. via spontaneous emission. Here, we theoretically study collective dipolar oscillations in finite planar atomic arrays in free space and analyze mechanisms that govern the emergence of subradiant collective states in such structures.

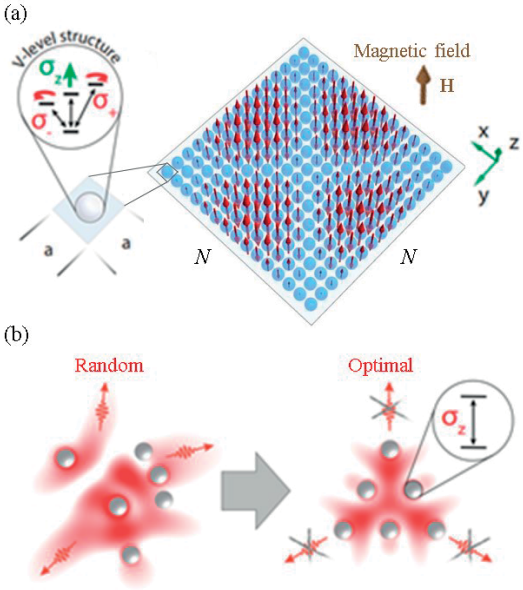

Fig. 1 (a) A two-dimensional finite square lattice of N atoms with V-level structure. Arrows show a snapshot of a wavefunction of the most subradiant state in a case of σ_z polarization of atomic transitions. (b) Two-level atoms are arbitrarly distributed in a plane z=0. Differential evolution method provides the optimal configuration of a system minimizing radiative losses for a given minimal interatomic distance $r_{min} \geq 0.38\lambda_0$.

In our research we consider identical two-level atoms with transition wavelength λ_0 and focus on the two cases: periodic two-dimensional arrays with total amount of atoms $N \geq 100$ [1] and arbitrary arrangement of a small number of atoms on a plane [2]. In the first case, we identify the main factors affecting the radiative losses suppression in such structures,

including interference of the out-of-phase oscillating neighbor dipoles in the far zone, external coupling of the states associated with the symmetry of the structure, and “accidental” external coupling that emerges due to quasi-flat polaritonic band dispersion of the corresponding infinite lattice. We establish the conditions under which these mechanisms are present and demonstrate the interplay between them on the example of the square array. Finally, we demonstrate that among different regular arrangements of the atoms the square atomic arrays support eigenstates with minimal radiative losses $\propto N^5$.

The results obtained for large regular atomic arrays, however, cannot be straightforwardly adapted to the small arrays. Therefore, for small structures ~10 atoms we utilized the differential evolution algorithm to find the optimal configurations that support the most subradiant eigenstates. Depending on the minimum allowed distance between the atoms, different quasi-regular structures turn out to be the optimal ones: one-dimensional chains, fragments of triangular, and square lattices. While the discovered weakly radiative configurations of small ensembles cannot be immediately predicted, there is a certain correspondence to the non-radiative states in the regular atomic lattices. Additionally, we show that for small interatomic distances the linear arrays with modulated spacing have the smallest radiative losses exponentially decreasing as the size of the ensemble increases.

This work was performed with financial support of the Russian Science Foundation (Project No.22-72-10047)

References

[1] I. Volkov, N. Ustimenko, D. Kornovan, R. Savelev, A. Sheremet, and M. Petrov, "Strongly subradiant states in planar atomic arrays," Nanophotonics **13** (3), 289-298 (2024).

[2] I. Volkov, S. Mitsai, S. Zhogolev, D. Kornovan, A. Sheremet, R. Savelev and M. Petrov, "Non-radiative configurations of a few quantum emitters ensembles: Evolutionary optimization approach," Appl. Phys. Lett. **124**, 084001 (2024).

Multi-level organization of carbon nanotubes for advanced THz optics

Raginov N.I.[1], Radivon A.V.[2], Ezersky A.S.[3], Chernykh A.V.[3], Terentyev A.V.[2], Zhivetyev K.V.[2], Rakov I.I.[1], Katyba G.M.[4,5], Novikov I.V.[1], Tsiplakova E.G.[3], Paukov M.I.[2], Starchenko V.V.[2], Arsenin A.V.[2], Spector I.E.[4], Kuznetsov S.A.[6], Zaitsev K.I.[4], Petrov N.V.[3], Burdanova M.G.[2,4], Kopylova D.S.[1], Gorshunov B.P.[2], Volkov V.[2], Nasibulin A.G.[1], Krasnikov D.V.[1]

[1] *Skolkovo Institute of Science and Technology, Moscow, Russia*
[2] *Moscow Institute of Physics and Technology, Dolgoprudny, Russia*
[3] *ITMO University, St. Petersburg, Russia*
[4] *Prokhorov Institute of General Physics of the Russian Academy of Sciences, Moscow, Russia*
[5] *Institute of Solid State Physics of the Russian Academy of Sciences, Chernogolovka, Russia*
[6] *Novosibirsk State University, Novosibirsk, Russia*

The unique set of mechanical, electrical, and optical features of carbon nanotubes has inspired scientists and engineers for several decades to create new materials and devices in various fields of our civilization: from medicine to aerospace, from telecommunications to construction technologies. Significant progress in the field of functional materials ensures the gradual introduction of nanotubes into such scientific and technological products as antistatic coatings, lithium-ion batteries and polymer composites; nevertheless, the development of carbon nanotube-based devices in optoelectronics and biomedicine lacks in performance. This is mostly related to insufficient control on nanotube properties. Here we report our recent advances on tuning carbon nanotubes to create an element base in the THz range. By identifying five levels of material organization ("individual nanotubes" [1, 2], "nanotube agglomerates" [3], "network of agglomerates" [4], "structured assembly" [5, 6], "system of assemblies" [7]), we transform the polyphony of properties of carbon nanotubes to THz create modulators, sensors etc.
The authors thank the joint Skoltech-MIPT-ITMO program "Clover".

[1] Maria G. Burdanova, Gleb M. Katyba, Reza Kashtiban, *et al.* (2021). Ultrafast, high modulation depth terahertz modulators based on carbon nanotube thin films *Carbon* **173**, 245-252
[2] Daria S. Kopylova, Daria A. Satco, Eldar M. Khabushev, *et al.* (2020). Electrochemical enhancement of optoelectronic performance of transparent and conducting single-walled carbon nanotube films. *Carbon* **167**, 244-248
[3] Novikov I.V., Krasnikov D.V., Vorobei A.M., *et al.* (2022). Multifunctional elastic composites with extremely low concentrations of single-walled carbon nanotubes *ACS applied materials and interfaces* **14**, 18866–18876
[4] Maksim I. Paukov, Vladimir V. Starchenko, Dmitry V. Krasnikov, *et al.* (2023). Ultrafast opto-mechanical terahertz modulators based on stretchable carbon nanotube thin films. *Ultrafast Science* **3**, 1-9
[5] G. M. Katyba, N. I. Raginov, E. M. Khabushev, *et al.* (2023). Tunable THz flat zone plate based on stretchable single-walled carbon nanotube thin films. *Optica* **10**, 53-61
[6] Ilya V. Novikov, Nikita I. Raginov, Dmitry V. Krasnikov, *et al.* (2024). Fast liquid-free patterning of SWCNT films for electronic and optical applications. *Chemical Engineering Journal* **485** 149733-149732
[7] Arina V. Radivon, Gleb M. Katyba, Nikita I. Raginov, Aleksey V. Chernykh, *et al.* (2024). Expanding THz vortex generation functionality with advanced spiral zone plates based on single-walled carbon nanotube films. *Advanced Optical Materials* **in press** https://doi.org/10.1002/adom.202303282

Mid-infrared photo-detector based on double quantum well structure

S. Yegiyan[1*], O. Klimenko[1], V. Antonov[1]

[1]Skolkovo Institute of Science and Technology, Moscow, 121205, Russian Federation, Moscow, Russia

**e-mail address: Samvel.yegiyan@skoltech.ru*

The methods of single-photon counting have been established across various spectral regions, such as X-ray, UV, visible, and near-infrared, to detect extremely faint radiation. These sensitive devises have extended the horizons for many branches of material science, biology, astrophysics, and photonics. However, in the long-wavelength range ($\lambda > 10\mu m$, frequencies lower than 30 THz) the photon energies are much smaller ($h\nu < 124$ meV for $\lambda > 10\mu m$), which makes single-photon detection significantly challenging [1]. Nevertheless, the MIR - THz region is a rich area of spectroscopy, covering rotational and vibrational spectra of molecules, liquids, and solids, as well as electron energy spectra in semiconductor nanostructures and the superconducting energy gap in metals. Therefore, the technology of sensitive microscopy with high spatial resolution in this spectral region would offer a powerful tool for investigating various materials and observing of fine physical effects.

In the past decade, several innovative detection schemes have been proposed. However, most solutions rely on extremely low temperatures close to 0,15 K. In this respect, photosensitive field-effective transistors created in a double quantum well (DQW) structures, also known as a CSIP, tends to be the most promising technology for feasible devices at conventional cryogenic temperatures (4.2-77K) [2]. Although the DQW technology, proposed a decade ago, is not yet sufficiently explored, several laboratory applications have been already developed. For instance, a near-field scanning microscope has been successfully engineered to investigate thermal radiation without external illumination [3]. It is highly likely that the scope of applications for this technology will significantly broaden in the future. Our research is aimed at the development of a compact MIR microscope based on closed cycle cryogenic setup and investigate sensitivity limits at comparably affordable temperature regimes (7-77K).

In general, the detectors perform as photo sensitive field effective transistor with floating gate (fig. 1.(a)). The isolation of upper QW from the source-drain channel, which is necessary for the operation, is served by gate electrodes. Once an electron in the isolated island (confined between gate electrodes) of the upper QW is exited from the ground state by the photon of resonance energy, it tunnels through the barrier and relaxes at the lower QW. Missing one electron, the isolated QW island becomes positively charged up by +e and serves as the floating gate to the conductance channel, so the intensity of incident radiation can be calculated by the conductance measurements.

During the research, we developed the fabrication process of fully functional CSIP detectors with resonance wavelength around 15 microns (fig.1(b)). The devices were fabricated by electron beam lithography within the GaAs heterostructures. The properties of samples were characterized by transport measurements at closed cycle cryocooler setup at temperatures from 7 to 300 K. We measured the photo response and sensitivity exploiting homemade BBR (Black Body Radiation) source(fig.1.(c)). Also, we designed and assembled a compact copper unit with an integrated confocal focusing system of Ge lenses, for proper shielding from the background radiation

We have succeeded in the fabrication of MIR detectors, operable under laboratory conditions. The source and drain contacts, deposited by magnetron with further annealing [4], managed to interconnect both layers of two-dimensional electron gas without distortion of the initial band structure. The electronic measurements were conducted with both commercial

Lock-in amplifiers and custom differential amplifier, which can be miniaturized in the future for standalone device. At 7 K, we observed well-defined photo response on the radiation emitted by the metal-film resistor heated to 50K (fig.1.(c,d)). Performed calculations proofed theoretically predicted sensitivities with NEP (Noise Equivalent Power) values around 10^{-18}, that is 2 orders of magnitude better than the closest alternatives in the spectral range. The advanced gating technique allows us to suspend the responsivity up to 20 K without a dramatic drop in sensitivity of the samples. The further research implies the direct measurements of spectral response and broadening the operation temperature range.

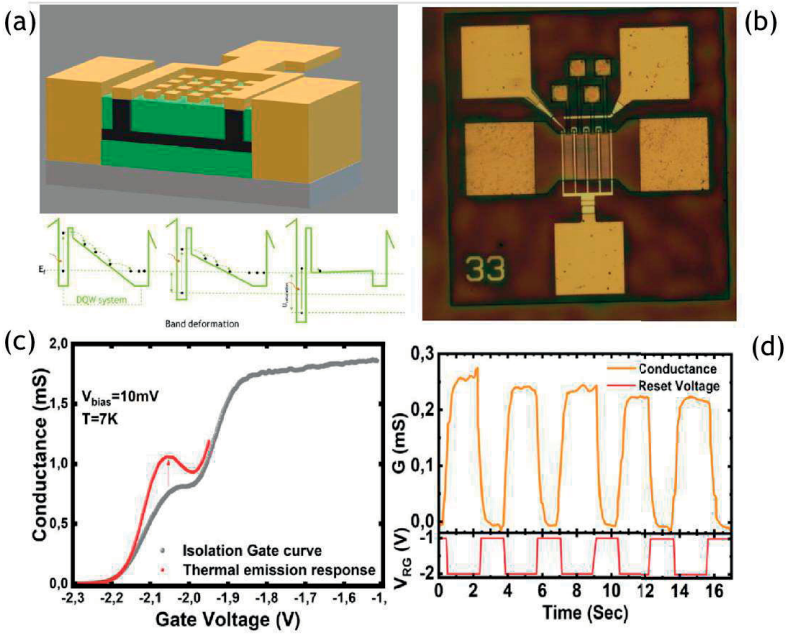

Fig. 1 . a) Schematic model of CSIP devise; b) Photo of fabricated device; c) Isolation curve at 7K. The red line corresponds to the photo response; d) Reset operation under illumination.

References

[1] Kun Huang, Yinqi Wang, Jianan Fang, Weiyan Kang, Ying Sun, Yan Liang, Qiang Hao, Ming Yan, and Heping Zeng, "Mid-infrared photon counting and resolving via efficient frequency upconversion," Photonics Research, vol. 9, no. 2, p. 259-265, January 2021

[2] Ueda, Takeji & Komiyama, Susumu, "Novel Ultra-Sensitive Detectors in the 10–50 μm Wavelength Range," Sensors, vol. 10, p. 8411-8423, September 2010

[3] Yusuke Kajihara, Keishi Kosaka, and Susumu Komiyama, "Thermally excited near-field radiation and far-field interference," Optics Express, vol. 19, p. 7695-7704, April 2011,

[4] Tao Lin, Jianan Xie, Shaohuan Ning, Zekun Ma, Yan Mu, WanJun Sun, Sha Yang, "Effect of annealing process parameters on N-GaAs ohmic contacts," Microelectronics Engineering, Vol. 258, April 2022

Terahertz-infrared spectroscopy of endofullerene [Li@C_{60}](PF_6)

S.S.Zhukov[1]*, A.V.Melentev[1], D.Yulamanova[1], N.Orekhov[2], P.Zhilyaev[3], E.S.Zhukova[1], S.Aoyagi[4], H. Suzuki[5], M. Nakano[6], B.P.Gorshunov[1]

[1]Laboratory of Terahertz Spectroscopy, Center for Photonics and 2D Materials, Moscow Institute of Physics and Technology (National Research University), Dolgoprudny, 141701, Moscow, Russia

[2]Moscow Institute of Physics and Technology (National Research University), Dolgoprudny, 141701, Moscow, Russia

[3] Center for Materials Technologies, Skolkovo Institute of Science and Technology, 121205 Moscow, Russia

[4]Department of Information and Basic Science, Nagoya City University, Nagoya 467-8501, Japan

[5]Department of Chemistry, Kindai University, 3-4-1 Kowakae, Higashiosaka, Osaka 577-8502, Japan

[6]Research Center for Thermal and Entropic Science, Graduate School of Science, Osaka University, Toyonaka, Osaka 560-0043, Japan

**e-mail address: zs1978@mail.ru*

Endofullerenes are attractive objects to study the properties of atoms and/or molecules under nano-confinement conditions, when the material properties can be cardinally different from those in the bulk form. On the other hand, from the viewpoint of possible applications, endofullerenes are perspective for use in various fields, including nano-electronics, hydrogen storage materials, biology, medicine and astrophysics. Here, we present the results of the detailed spectroscopic studies of the metallofullerene Li@C_{60} synthesized with PF_6 counter anions. This system is attractive due to a complex multi-well potential experienced by the Li ion within the C60 nano-cage: theory predicts 20 shallow potential minima [1] between which Li can hop or tunnel. We have performed detailed terahertz-infrared (frequencies 5-700 cm^{-1}) spectroscopic studies of the [Li@C_{60}](PF_6) complex at temperatures 5-300 K, with measurements made in fine temperature steps, 5 to 10 K. We observe a rich set of absorption resonances, see Figure 1. Processing the observed absorption lines with the Lorentzian expressions allowed us to obtain the detailed quantitative information on the temperature behaviors of the frequency positions of the lines, on their intensities and damping factors. The temperature behavior of these parameters reveals anomalies around the temperature of ≈25 K of an antiferroelectric phase transition in the system of interacting Li^+/PF^-_6 dipoles [2,3], and at temperatures 100 – 120 K, when Li ions begin to condense within the potential wells of localizing potential within the C60 cage [2,4]. A number of the observed resonances exhibit pronounced isotopic frequency shifts, indicating the involvement of Li ions in the corresponding vibrational processes. Signatures of excitation at ≈6 cm^{-1} are detected, which can be related to the transition between tunnel-split energy levels of localized lithium ions. The assignment of the absorption resonances is performed based on the temperature variation of the lines' parameters, the isotopic frequency shifts and on computer simulations.

Acknowledgement

The terahertz-infrared experiments and spectral analysis were supported by RFS grant 23-22-00105.

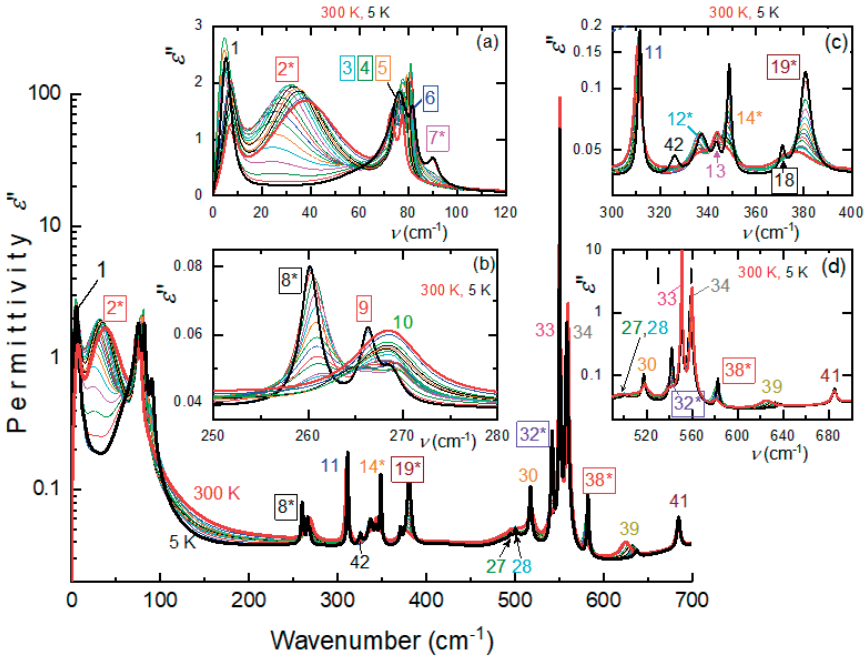

Fig.1 Terahertz-infrared spectra of imaginary dielectric permittivity of [^{6}Li@C_{60}](PF_6) measured at several temperatures. Absorption lines observed in "pure" C60 are not shown. Lines are numbered according to their growing frequencies. Stars mark lines that are strongly dependent on temperature. Numbers in boxes mark lines that show isotopic shifts when ^{6}Li in [^{6}Li@C_{60}](PF_6) is replaced by ^{7}Li. Vertical bars in inset (d) indicate PF_6 intramolecular vibrations at 530 cm^{-1} and 559 cm^{-1}.

References

[1] M.Zhang, L.B. Harding, S.K. Gray, S.A.Rice, "Quantum States of the Endohedral Fullerene Li@C60", J0urnal of Physical Chemistry A, **112**, 5478 (2008).

[2] S.Aoyagi, A.Tokumitu, K.Sugimoto, H.Okada, N.Hoshino, T.Akutagawa, "Tunneling Motion and Antiferroelectric Ordering of Lithium Cations Trapped inside Carbon Cages", Journal of the Physical Society of Japan, **85**, 094605 (2016).

[3] Hal Suzuki, Misaki Ishida, Chiko Otani, Kazuhiko Kawachi, Yasuhiko Kasama, Eunsang Kwon, Yuji Miyazaki and Motohiro Nakano, "The thermodynamic properties and molecular dynamics of [Li^+@C60](PF_6-) associated with structural phase transitions", Physical Chemistry Chemical Physics, **21**, 16147 (2019).

[4] S.Aoyagi, Y.Sado, E.Nishibori, H.Sawa, H.Okada, H.Tobita, Y.Kasama, R.Kitaura, H.Shinohara, "Rock-Salt-Type Crystal of Thermally Contracted C60 With Encapsulated Lithium Cation", Angewandte Chemie International Edition, **51**, 3377 (2012).

Suppression of superconductivity in thin MoRe films

E. S. Zhukova[1], B. M. Nekrasov[1], L. S. Kadyrov[1], A. V. Melentev[1], A. S. Shaimardanov[1,2], A. G. Shishkin[1,2,3], A. A. Golubov[4], M.Yu. Kupriyanov[2,5], B. P. Gorshunov[1*], V. S. Stolyarov[1,2,3]

[1]Moscow Institute of Physics and Technology (National Research University), 141700 Dolgoprudny, Russia

[2]National University of Science and Technology (MISIS), 119049 Moscow, Russia

[3]Dukhov Research Institute of Automatics (VNIIA), 127055 Moscow, Russia

[4]Faculty of Science and Technology and MESA+ Institute for Nanotechnology, University of Twente, 7500 AE Enschede, Netherlands

[5]Skobeltsyn Institute of Nuclear Physics, Lomonosov Moscow State University, 119991 Moscow, Russia

**e-mail address: bpgorshunov@gmail.com*

Molybdenum-rhenium superconducting alloys continue to attract the attention of researchers from a fundamental viewpoint because of their intriguing properties in the superconducting (SC) state and their potential for use in modern electronics. We have carried out the first detailed and systematic measurements and analyses of the electrodynamic properties of $Mo_{0.6}Re_{0.4}$ films with various thicknesses (10 to 100 nm) prepared by magnetron sputtering. Experiments were performed at frequencies of 0.15 – 2.4 THz (wavenumbers 5 - 80 cm^{-1}) and at temperatures of 5-300 K, using terahertz time-domain spectrometer. Spectra of the complex transmission coefficient of the films on highly-resistive silicon substrates were measured and processed to obtain frequency-temperature-thickness-dependent parameters of the films in the normal and SC states. The main results are summarized in Figure 1, where the dependence of the London penetration depth, the SC critical temperature and the SC energy gap are shown as a function of films thickness. The temperature dependence of the superconducting energy gap, the penetration depth, the superconducting condensate plasma frequency and the normalized superfluid density are reproduced within the two-fluid superconductivity model. A strong decrease in the critical temperature and the SC energy gap in the films is ascribed to the suppression of the mean superconducting order parameter due to a decrease in the local electronic density of states in the films near their surfaces. The ratio $2\Delta(0)/k_BT_c = 3.8\pm0.2$ for all films is found to slightly exceed the BCS value 3.52, indicating moderately strong electron-phonon coupling. We show that MoRe alloy is a perspective material for the design of elements and devices of advanced electronics and optoelectronics, e.g., single photon detectors or high-Q resonators for frequency locking systems.

Acknowledgements

This work was supported by RSF 23-72-30004 (terahertz experiments and data analysis). Magnetron sputtering films fabrication was supported by the Ministry of Science and Higher Education of the Russian Federation (No. FSMG-2022-0014).

References

[1] S.Maekawa, H.Fukuyama, “Localization effects in two-dimensional superconductors”, J. Phys. Soc. Japan, **51**, 1380 (1982).

[2] G. Simonin, “Surface term in the superconductive Ginzburg-Landau free energy: Application to thin films”, Phys. Rev. B, **33**, 7830 (1986).

[3] A.M.Finkel'shtein, “Superconducting transition temperature in amorphous films”, JETP Lett., **45**, 37 (1987).

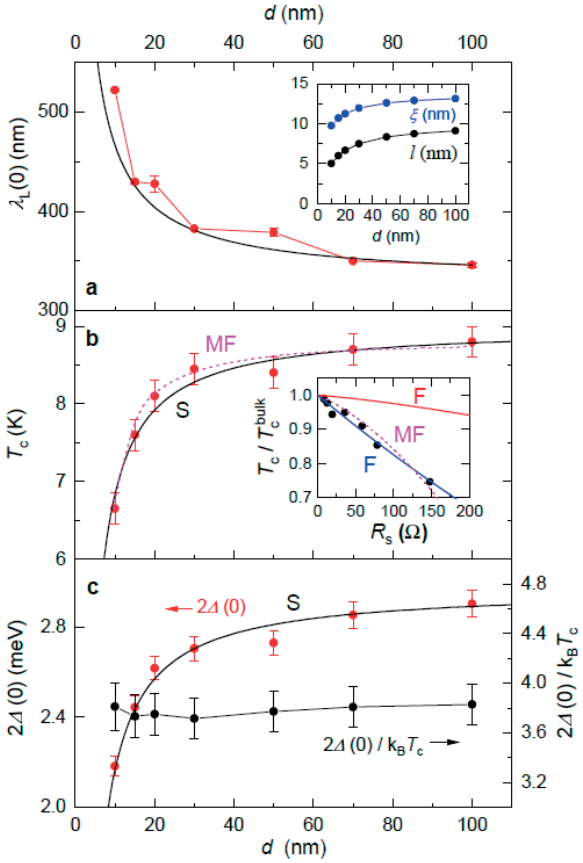

Fig. 1 Thickness (d) dependence of the zero-temperature London penetration depth (a), the critical temperature (b), the superconducting energy gap and the ratio $2\Delta(0)/k_BT_c$ (c) for $Mo_{0.6}Re_{0.4}$ films. In panel b, the dashed line (labelled MF) is a result of calculation according to the expression (29) from [1] and solid line (labelled S) corresponds to the least-square fit with the expression (8) from [2]. In panel c, the solid line (labelled S) shows a fit with $2\Delta(d)\sim(1-\text{const}/d)$. Inset in panel a: thickness-dependent coherence length and electron mean free path. Inset in panel b: dots - the dependence of the critical temperature of $Mo_{0.6}Re_{0.4}$ films on their surface resistance; dashed line (labelled MF) - least-square fit with expression (29) from [1]; blue line (labelled F) - fit according the expression (5) from [3]; red line (labelled F) - calculation using the expression (29) from [1] with the same parameters as before, but with the thickness-dependent mean free path, see inset in panel a.

Chiral photonic crystals and metamaterials for compact sources of circularly polarized light

S. G. Tikhodeev

Lomonosov Moscow State University, Department of Physics

Prokhorov General Physics Institute, Russian Academy of Sciences

The development of compact sources of circularly polarized light that do not require the application of a static magnetic field and macroscopically-thick quarter-wave plates has recently attracted much research attention. Such sources can be very useful in spectroscopy and sensorics, including bio-sensorics, as well as in spintronics. In my talk I will discuss the principles of operation of such devices based on chiral photonic crystals and metamaterials. A chiral photonic crystal slab made of GaAs on AlGaAs planar waveguide with embedded InAs quantum dots is the first successful device of this kind [1]. Another interesting example are lasers based on semiconductor microcavities with chiral photonic crystal manufactured on the cavity top mirror and with light-emitting GaAs quantum wells in the active region, under optical [2] and electrical [3] pumping. Common for such structures is the fabrication of specially optimized chiral photonic crystal layers with C4 rotational symmetry from rectangular micropillars on their top surface. Polarization optical filters based on chiral metasurfaces [4,5] as well as circularly polarized photon routers for spintronics [6] will also be discussed.

The work was supported by Russian Science Foundation (project No. 22-12-00351).

[1] S. V. Lobanov et al., Phys. Rev. B **92**, 205309 (2015).
[2] A. A. Demenev et al., Appl. Phys. Lett. **109**, 171106 (2016).
[3] A. A. Maksimov et al., Phys. Rev. Appl. **17**, L021001 (2022).
[4] B. Semnani et al., Light-Sci. Appl. **9**, 23 (2020).
[5] K. Voronin et al., ACS Photonics **9**, 2652 (2022).
[6] S. A. Dyakov et al., Phys. Rev. Appl. **14**, 024090 (2020).

Научное издание

RESONANT NANOPHOTONICS 2024
EDUCATIONAL WORKSHOP

July 8–12, 2024, Moscow

Book of abstracts

Electronic edition of network distribution

The text is printed in the author's edition

РЕЗОНАНСНАЯ НАНОФОТОНИКА — 2024
ОБРАЗОВАТЕЛЬНЫЙ СЕМИНАР

8–12 июля 2024 года, Москва

Тезисы докладов

Художественное оформление *К. В. Саутенков*
Верстка, подготовка иллюстраций *Е. В. Холмогорова*

Электронное издание сетевого распространения

Текст печатается в авторской редакции

Макет утвержден 02.12.2024. № 12910.

Издательство Московского университета

119991, Москва, ГСП-1, Ленинские горы, д. 1, стр. 15
Тел.: (495) 939-32-91; e-mail: secretary@msupress.com
https://msupress.com. Отдел реализации:
тел.: (495) 939-33-23; e-mail: zakaz@msupress.com